Neutrino experiments at high energies

P. F. Ermolov and A. I. Mukhin

Institute of High-Energy Physics, Serpukhov (Moscow oblast')
Usp. Fiz. Nauk **124**, 385–440 (March 1978)

A review ø is given of experimental work in the field of neutrino physics carried out between 1972 and the first half of 1977 using high energy accelerators. The methodology of neutrino experiments is examined including neutrino beams, modern electronic detectors, and bubble chambers. Data are presented on the measurement of total cross sections with charged and neutral currents. Results of studies of elastic and deep inelastic scattering and their theoretical interpretation are described. The principal mechanisms of production of new particles and the results of an experimental search for them in neutrino interactions are discussed.

PACS numbers: 13.15.+g, 12.30.−s

CONTENTS

1. INTRODUCTION

This review pursues the aim of systematizing the experimental studies in the field of neutrino physics that have been performed in the last several years (1972–1977) using high-energy accelerators.

Neutrino experiments were first carried out in the early sixties using the accelerators of the Brookhaven National Laboratory (USA)[1] and of CERN.[2] These experiments led to the discovery[1] that the neutrino that appears in decay reactions together with electrons (ν_e) is a different particle from the neutrino associated with the muon (ν_μ). These experiments and subsequent ones using bubble chambers[3] have shown that all the fundamental characteristic features of the interaction of neutrinos with nucleons (linear increase with energy of the total cross section, differing interaction cross sections of neutrinos and antineutrinos, local nature of the interaction, conservation of muon charge, production of mesons) satisfy well the universal four-fermion V–A theory of weak interactions with the $SU(3)$ symmetry of strong interactions taken into account.[4,5]

Being particles that do not possess strong and electromagnetic charges, the neutrinos seem at present to be practically the only possibility for studying the weak interactions at high energies.

The topicality of these studies has become even more

 0038-5670/78/030185-30$01.10

evident after a number of experimental discoveries and considerable advances in the theory of elementary particles that have been made in the last few years.

In 1967 Weinberg and Salam[6] proposed a minimal renormalizable gauge-invariant model of the weak and electromagnetic interactions (the WS model). This model stemmed from numerous theoretical studies of spontaneously broken symmetry groups of elementary particles and attempts to universalize the strong, weak, and electromagnetic interactions.[7, 174]

The WS model[175] introduced a gauge-invariant group in which the gauge vector fields form a triplet of the $SU(2)$ group and a singlet of the $U(1)$ group. They interact with two types of lepton fields: one that corresponds to left-helical leptons combined into a $SU(2)$ doublet, and the other to right-helical charged leptons combined into a $U(1)$ singlet. Here the muonic and electronic lepton charges are conserved separately. The photon field is a linear combination of two neutral fields of the singlet and the neutral component of the triplet: It corresponds to the unbroken symmetry subgroup involved with conservation of electric charge, whereas the orthogonal linear combination of the fields corresponds to a neutral intermediate Z-boson. The other gauge fields form the field of the heavy intermediate charged $W^{\pm}$ bosons. The two neutral fields are coupled by different constants g and g' to the "weak" isotopic spin T and the "lepton" hypercharge $Y = T_3 - Q$. Breaking of $\gamma - Z$ symmetry arises from spontaneous breaking of the $SU(2) \cdot U(1)$ group by the Higgs scalar non-strongly-interacting particles and this is responsible for the masses of the intermediate bosons. The constants g and g' are linked by the relationship $\tan\theta_W = g'/g$, $e = g\sin\theta_W$, where θ_W is the unknown mixing angle (the Weinberg angle). The WS model leads to important consequences.

In this case the theory is renormalizable and it proves possible to employ perturbation theory in any order and to make definite predictions within the framework of a chosen scheme. As we know well, the old theory contains fundamental difficulties. For example, in the four-fermion reaction[4]

$$\nu_\mu + e^- \to \nu_e + \mu^-,$$

which occurs only via the s-state, the cross section as expressed in terms of the momentum P_ν of ν_μ in the center-of-mass system has the form

$$\sigma = \frac{4}{\pi}(GP_\nu)^2,$$

where G is the Fermi constant. Since the unitarity condition implies that $\sigma < (\pi/2)\lambda^2$, the expression given above holds only when $P_{\nu_\mu} < 300\,\text{GeV}/c$. At these energies in the Fermi theory one must account for all the higher orders of perturbation theory.[9] In the WS model one should see a change in regime of the energy-dependence of the cross section at energies in the center-of-mass system of the order of the masses of W and Z. The latter are defined as follows in terms of $\sin\theta_W$:

$$m_W = \frac{2^{-5/4}G^{-1/2}e}{\sin\theta_W} = \frac{37.3}{\sin\theta_W}\,\text{GeV},\quad m_Z = \frac{74.6}{\sin 2\theta_W}\,\text{GeV}.$$

When $\sin^2\theta_W = 0.35$, we have $m_W = 63\,\text{GeV}$, $m_Z = 77\,\text{GeV}$.

Production of particles of this mass and verification of a change in regime of the energy-dependence of the cross sections is not yet possible with modern accelerators ($\sqrt{s} \leq 20\,\text{GeV}$). Apparently this will become possible in the next few years using new accelerators with colliding proton beams of energy $E \geq 200\,\text{GeV}$.

A direct proof of the gauge-invariant theory would be the discovery of a Higgs meson. However, as analysis shows,[10] experimental detection of such particles is very difficult at present owing to their large mass (a few GeV or even $\geq 10\,\text{GeV}$) and relatively small interaction cross section.

The WS model naturally implies the existence of neutral currents in the weak interaction. Hence they have become the object of intensive experimental searches, and they were actually discovered in $\nu_\mu N$ and then in $\nu_\mu e$ scattering. Shekhter[93] has reviewed the first experimental studies on neutral currents.

The detailed study of neutral currents in neutrino experiments is currently one of the pressing problems of modern elementary particle physics.

Yet perhaps the most important merit of the gauge-invariant theory is the possibility of establishing a deeper symmetry between the leptons and the hadrons. Here, in addition to the three quarks (u, d, and s) that constitute all the known strongly-interacting particles that correspond to $SU(3)$ symmetry, we also need a fourth quark that has the same charge as the u quark, but differs from it by a new quantum number. The new quantum number charm (c) takes on the values ± 1 and is conserved in strong and in electromagnetic interactions but is not conserved in weak interactions.[1)] In the scheme proposed by Glashow, Iliopoulos, and Maiani (GIM),[12] all the strongly-interacting particles consist of four quarks: of left-helical isodoublets and of right-helical isosinglets. Now one has the symmetry

$$\begin{pmatrix}\nu_\mu\\ \mu^-\end{pmatrix}_L,\quad \begin{pmatrix}\nu_e\\ e^-\end{pmatrix}_L,\quad \begin{pmatrix}u\\ d'\end{pmatrix}_L,\quad \begin{pmatrix}c\\ s'\end{pmatrix}_L,$$

where the fields are $d' = d\cos\theta_C + s\sin\theta_C$ and $s' = -d\sin\theta_C + s\cos\theta_C$, and θ_C is the Cabibbo angle, which from experiment is equal to $\sim 15°$. This symmetry allows one to remove one of the main difficulties in applying the WS model to weak processes with change in strangeness that occur via neutral currents. In the WS model with a scheme of only three quarks, the probability of the processes $K^0 \to \mu^+\mu^-$, $K^+ \to \pi^+\nu\bar{\nu}$, etc.) as well as the mass difference of the states of the K^0 meson, $K_1^0 - K_2^0$, turns out to be 5–6 orders of magnitude larger than the observed quantities. In the GIM scheme[12] with four quarks, owing to the fact that the two quark doublets enter into the weak current symmetrically, it turns out that the neutral currents with conservation of strangeness remain, but those with a change in strange-

[1)] The new quantum number "charm" was introduced into the theory considerably earlier and was associated with a scheme of quarks of integral charge (see, e.g., Ref. 11).

ness vanish in any order of the theory of the weak interaction. In order that such compensations should not be broken down by the strong interactions, the latter must be symmetrical with respect to the two quarks c and u. In combination with the $SU(3)$ symmetry of the three quarks that is invariant with respect to strong isotopic spin, this leads to the requirement of $SU(4)$ symmetry. Owing to the difference in the mass of the quarks, this symmetry is only approximate, and the mass relationships in the lowest order of $SU(4)$ symmetry are considerably more strongly violated than in $SU(3)$ symmetry. The $SU(4)$ symmetry leads to prediction of new baryon and meson multiplets, which in addition to the usual particles and resonances include also new pseudoscalar and vector mesons with the open quantum number $c = \pm 1$ or 0 (bound states $c\bar{c}$), and of baryons having $c = 1, 2$.[13]

Two experiments in 1974 (with colliding electron-positron beams[14] and in hadron interactions[15]) resulted in the simultaneous discovery of a heavy ($m = 3095\ \text{MeV}/c^2$) vector meson that is relatively stable on the nuclear scale ($\tau \geq 10^{-20}$ sec). It has been designated as the J/ψ-particle. The interpretation of this meson as the bound state $c\bar{c}$, together with further studies of other states in this mass region ("charmonium" levels), have placed on the agenda the problem of seeking particles having the open quantum number of charm.[16] Since we are dealing here with a new type of elementary particles unequalled since the time of discovery of the strange particles, experimental investigations along this line are being conducted at practically all modern high-energy accelerators.

The narrow peaks in the invariant masses of the neutral systems $K\pi\pi\pi$ and $K\pi$ and of the charged system $K^-\pi^+\pi^-$ that have been discovered relatively recently in the process of e^+e^- annihilation, as well as the corresponding peaks in the invariant mass of the recoil systems, are very likely candidates for the lightest pseudoscalar and vector charmed mesons D and D^*.[17, 177]

Neutrino experiments play a large role in the study of charmed particles, since one can expect a relatively large yield of them (~10%) in νN interactions. The effects of production of new particles have actually been observed, also starting in 1974.

Another important discovery made in the process of e^+e^- annihilation, namely the discovery of anomalous μe pairs, is interpreted as a possible pairwise production of new charged heavy leptons.[19, 176] If this interpretation is confirmed, this will imply the existence of an even more extensive system of quarks and a new hadron-lepton symmetry, since the current models[19, 20] that add to the c quark one or two new quarks (the b and t quarks) almost unavoidably lead to the existence of new heavy leptons. Searches for objects other than charmed particles, including heavy leptons, quarks, and colored gluons, are also promising in neutrino experiments.[21, 22]

Finally, the interactions of neutrinos with nucleons at high energies bear most directly on the study of the more general structure of nucleons in connection with the hypothesis of scaling and of the quark-parton models.[16, 23] As is well known, a scaling behavior of the scattering of electrons (or muons) by nucleons has been found at high energies in the so-called deep inelastic region (i.e., for large energy transfers ν_H to the hadron and large momenta Q^2 imparted to the lepton). The interaction cross sections have proved to depend only on the variable $x = Q^2/2m_N\nu_H$, rather than on each variable Q^2 and ν_H separately. One assumes in the parton model that if the interaction time is short, i.e., the transferred momentum is large in comparison with the characteristic hadron masses, the virtual photon sees the nucleon as though consisting of point particles, or partons. If the nucleons have the momentum P_N, then the partons have a fraction of it equal to $x \cdot P_N$, where x coincides with the scaling variable introduced above, as we see from the kinematics of the elastic scattering. Then the probability of interaction is proportional to the distribution function of the partons in the nucleon with respect to the variable x, multiplied by the square of the charge of the parton, this being associated with the exchange of a virtual photon. One further assumes that the partons bear the quantum numbers of the quarks. For example, an essential point is that the half-integral spin of the partons stems from the smallness of the longitudinal cross section in eN scattering. A distinction is made between valence partons (for nucleons, u and d quarks) and the "sea" of parton-antiparton pairs ($u\bar{u}, d\bar{d}, s\bar{s}, c\bar{c}$). The latter involves the fact that the treatment of the nucleon as a bound state of three quarks is valid only in the nonrelativistic approximation. Virtually the nucleon transforms into a state having a large number of quarks. The time of these fluctuations is small, and hence they are important only in the deep inelastic processes. Qualitative considerations imply that the smaller is the value of x for fixed Q^2, the larger is the mass of the virtual states. Hence it is precisely at small x that one can naturally expect a large contribution from the "sea" of parton-antiparton pairs. We also know from experiment that the partons possess only about one-half of the momentum of the nucleon, while neutral gluons carry away the rest of the momentum. One assumes that the gluons are vector particles that do not bear quantum numbers of the types of isospin, strangeness, and charm, and which do not participate in weak nor electromagnetic interactions; the gluons give rise to the strong interactions between the quarks.

In the "color" theories of quarks[16, 24] (the new quantum number "color" can adopt three values, e.g., red, blue, and yellow, and it is needed to make the spin and the quark statistics agree), the forces acting between the quarks become small at small distances. That is, the particles act as though free at large momentum transfers ("asymptotic freedom").[25] This makes possible a theoretical explanation of the scaling hypothesis in the deep inelastic region, and it allows one to calculate by field theory technique (e.g., by perturbation theory) the corrections to the scaling behavior of the cross-sections, which are proportional to the coupling constant of the gluons with the quarks and to the logarithm of Q^2. The process of deep inelastic scattering of neutrinos by nucleons is treated in the parton model

by analogy with the electromagnetic interactions by replacing the virtual photons with the W-boson and introducing an additional form factor associated with the $V-A$ nature of the weak interactions. The study of the overall structure of the nucleon in νN interactions at high energies in the scaling variables x and y (y is the relative energy transfer, $y = \nu_H/E_\nu$) is of great interest, and one can treat any deviations from scaling behavior as new phenomena involving, in particular, the creation of new particles.

Thus we see from a brief presentation of the fundamental modern theoretical approaches to the processes of interaction of neutrinos with nucleons or leptons their important role in studies of elementary-particle physics.

2. METHODOLOGY OF NEUTRINO EXPERIMENTS

a) Neutrino beams from accelerators

The source of neutrinos (or antineutrinos) coming from accelerators is the lepton decay of unstable particles that are formed by interactions of the primary beam of accelerated protons with the nucleons of the target material.

The bulk of the high-energy neutrinos comes from the two-particle decays of charged pions and kaons:

$$\left\{\begin{matrix}\pi\\K\end\right\}^+ \to \mu^+ + \nu_\mu, \quad \left\{\begin{matrix}\pi\\K\end\right\}^- \to \mu^- + \bar{\nu}_\mu.$$

The most prominent contribution to the neutrino flux, which must be taken into account at the current level of conduct of experiments, comes also from three-particle decays of charged and neutral kaons:

$$K \to \mu + \nu_\mu + \pi, \quad K \to e + \nu_e + \pi.$$

Usually the fraction of neutrinos from three-particle decays lies at the 1% level, and it depends on the scheme adopted for producing the neutrino beam.

We see that from accelerators one gets beams of muon-type neutrinos. This determines the fact that the interaction properties of electron-type neutrinos have practically not been studied up to now.

Figure 1 shows a diagram illustrating the production of neutrino beams. The depicted scheme of production of a neutrino beam is based on a proton beam taken from

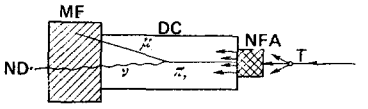

FIG. 1. General diagram of the production of a neutron beam. p—proton beam, T—target, NFA—neutrino-focusing apparatus, DC—decay channel, MF—nuon filter, ND—neutrino detectors.

an accelerator, which is focused on the target T. The mesons produced in the target pass through a neutrino-focusing apparatus. The construction details of the focusing apparatus depend on the properties of the neutrino beam that one wishes to obtain. Here mesons of the desired sign in a selected range of angles and momenta are focused into a nearly parallel beam (mesons of the opposite sign are defocused) and directed into a "decay" channel—a space where the mesons freely decay. The decay channel ends in a massive (in most cases steel) absorber, or muon filter. Here the remaining hadrons and muons produced in decay events are completely absorbed. Neutrino detectors are placed beyond the muon filter.

Table I and Figs. 2–4 give the fundamental characteristics of the neutrino beams.

1) Neutrinos with a broad energy spectrum. Such beams exist in all accelerators where neutrino studies are being performed,[26-30] and their chief advantage consists of the fact that they provide the highest neutrino fluxes.

One can show more concretely the production of a beam with a broad energy spectrum on the example of the neutrino channel of the Institute of High-Energy Physics (IHEP). The focusing apparatus consists of four parabolic lenses combined into three objectives, which are set up inside the target station.[31] The arrangement of the focusing apparatus and its optical characteristics for one of the flux regimes of the objectives are shown in Fig. 5. The angular acceptance of the system is as much as 60 milliradians. This means that the focusing system catches from 50 to 90% of the mesons emerging from the target in a momentum interval of 4–10 GeV/c, and almost completely catches the mesons of higher momenta. The defocused particles are absorbed by collimators in the radiation shielding of the target station. Figure 3 gives an example of the spectra of neutrinos and antineutrinos obtained in one of

TABLE I. Characteristics of neutrino channels and beams.

Accelerator	Proton energy, GeV	Method of beam production	Length of decay tunnel,m	Thickness of muon filter,m	I_p (per pulse)	Working neutrino energy range, GeV
ANL	12.4	Magnetic horn	30	13 (iron)	$1.2\cdot10^{12}$	0.3—6
CERN	26	» »	70	22 (iron)	$6\cdot10^{12}$	1—12 (Fig. 2)
BNL	29	» »	57	30 (iron)	Up to $5\cdot10^{12}$	1—15
IHEF	70	parabolic lenses	140 (vacuum)	62 (iron)	Up to $3.5\cdot10^{12}$	2—30 (Fig. 3)
FNAL	300—400	a) Magnetic horn b) Quadrupole triplet c) Monochromatization	340 (vacuum)	1000 (soil + iron)	Up to $1.5\cdot10^{13}$	10—200 (Fig. 4)
CERN SPS	400	a) Magnetic horn b) Monochromatization	300 (vacuum)	400 (iron)	$5\cdot10^{12}$	10—200

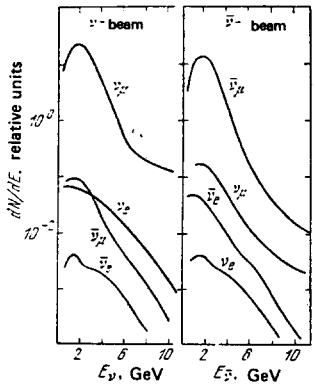

FIG. 2. Neutrino spectra for the CERN accelerator (E_p = 26 GeV).

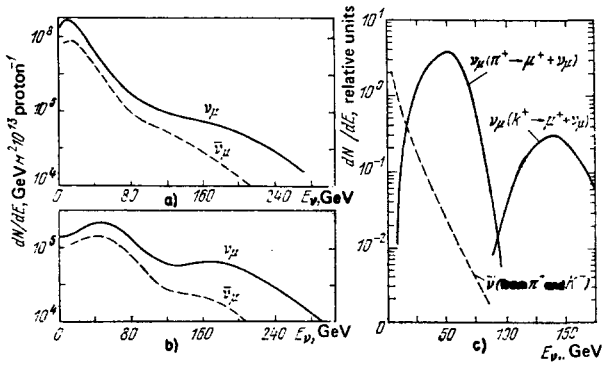

FIG. 4. Neutrino spectra for the FNAL accelerator (E_p = 300–400 GeV). a) Magnetic horn; b) quadrupole focusing; c) dichromatic beam.

the focusing regimes of the system.

This shape of the spectrum is typical of all accelerators. A sharp, almost exponential decline of the intensity with increasing energy is characteristic. The intensity of the antineutrino beam is smaller than that of the neutrino beam, especially in the high-energy region, which is governed by the decays of kaons. This is due to the fact that fewer negative mesons are produced in proton interactions than positive mesons.

The latter circumstance also has the effect that the admixture of neutrinos in an antineutrino beam attains a considerable magnitude, and at high energies it can even exceed the flux of antineutrinos if one doesn't take special measures against this. The use of an absorber set up behind the target along the axis of the beam substantially diminshes the undesired admixture of neutrinos of the other type, especially in the high-energy region, as we see from Fig. 6.

In some cases it is more convenient to operate with a less intense beam extended over time, which contains the natural ratio of neutrinos and antineutrinos. Such a beam has been realized in a very simple form in the Fermi National Accelerator Laboratory (FNAL) in the most recent experiments of the Harvard-Pennsylvania-Wisconsin-Fermi Laboratory group (HPWF).[32] In these experiments a triplet of quadrupole lenses was placed directly beyond the target. Particles that were produced in an angular range of $0<\theta<2$ milliradians with respect to the direction of the proton beam were focused. Figure 4b shows the calculated spectra of the neutrinos and antineutrinos produced by the triplet of quadrupoles (the momentum $p = 200\,\text{GeV}/c$ is focused).

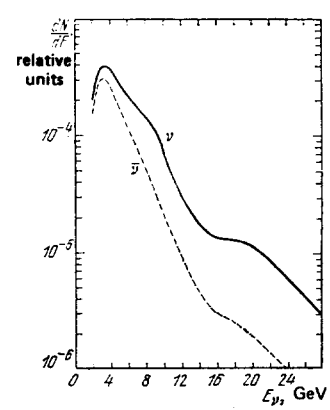

FIG. 3. Neutrino spectra for the IHEP accelerator (E_p = 70 GeV).

2) Monochromatized (dichromatic) beams. The urgent need to produce beams of monochromatized neutrinos is dictated primarily by the needs of investigation of neutral currents and study of lepton decays of the new particles. Moreover, a knowledge of the energy of the interacting neutrino substantially facilitates analysis of the studied processes in all cases.

The fundamental principle for producing beams of this type consists of the following. Beyond the target a narrow beam of hadrons of the desired sign and small angular divergence is produced with a small scatter in momenta. Then this beam is directed into the decay channel. The decaying π- and K-mesons give two "lines" that are separated in energy. One can vary the energy width of the neutrino "lines", depending on the relationship between the lengths of the decay channel and the shielding and the transverse dimensions of the neutrino detector. As an example, for a monochromatic parallel beam of mesons of energy E_0, the energy width of the neutrino lines is fully determined by the polar angle θ_2 that the detector subtends from the end of the decay channel and by the gamma factor of the mesons ($\gamma_{\pi,k} = E_0/m_{\pi,k}$):

$$\frac{\Delta E_\nu}{E_\nu} = \frac{\gamma^2\theta_2^2}{1+\gamma^2\theta_2^2}$$

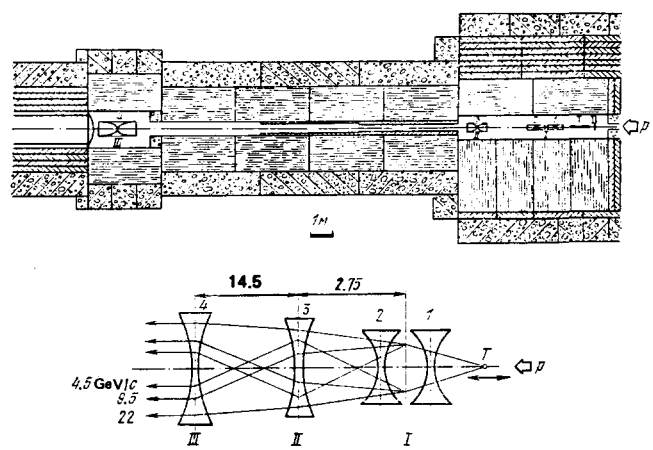

FIG. 5. Diagram of production of the neutrino beam at IHEP.

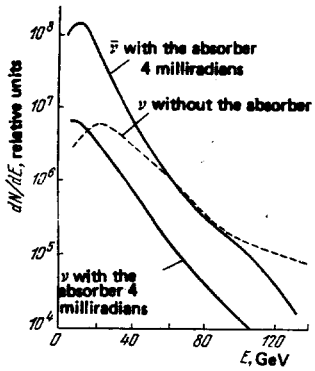

FIG. 6. Spectrum of $\bar{\nu}$ at FNAL and the ν admixture (with and without the absorber).

with the maximum energies $E_\nu = 0.95E_0$ (for the decay of a K-meson) and $E_\nu = 0.43E_0$ (for the decay of a π-meson). The energy width of the lines is also affected by the angular divergence of the meson beam and its momentum scatter.

Monochromatization of a neutron beam was first achieved in practice in the accelerator in Batavia by the joint experimental groups of the California Institute of Technology and the Fermi National Accelerator Laboratory (CITF). They used a rather broad range of momenta of the mesons (30%) so as to increase the intensity of the neutrino beam. Of course, this considerably increased the width of the energy spectrum of the neutrinos, as is shown in Fig. 4c.[33]

Beams of monochromatized neutrinos are beginning to be used in the new Superproton Synchrotron (SPS) at CERN (400-GeV energy of the proton beam).[34] In the first experiments,[153, 156] the momentum range of the produced meson beam amounted to $\Delta p/p = 0.10-0.14$ (full width at half-height) with an angular divergence of 0.3 milliradians horizontally and 0.6 milliradians vertically. For more exact determination of the energy, they used information on the coordinate of the point of interaction in the detector with respect to the axis of the beam.

3) Methods of determining neutrino spectra. A feature of neutrino beams is that they are not subject to control in the course of the experiment. Hence, as a rule, all the stages in the production of the neutrino beam are controlled.[35]

The measurement, or more exactly the reconstruction, of the energy spectrum of neutrinos is a rather delicate problem. There are several approaches to solving it.

One can calculate the neutrino spectrum if one knows the momentum and angular distributions of the particles produced in the proton interactions with the real target that stands in front of the focusing system. Measurements of the yields of particles from a real target, which usually has the dimensions of 1–2 nuclear interaction lengths along the beam, present *per se* a rather complicated problem, which hasn't yet been fully solved for any accelerator. Additional uncertainties in calculating the neutrino spectrum are introduced by the interaction of the produced beam with the construction parts of the producing system. In working with dichromatic beams, gas Cerenkov counters are placed in the produced meson beam in order to determine the composition of the beam (K/π ratio).[155]

Another independent experimental method is that of reconstructing the neutrino spectrum from the measured distributions of the muon flux at different depths of the muon filter.

The muon spectrum to be measured inside the shielding is primarily determined by the decays of π-mesons.[36, 37] Hence one can directly reconstruct from the muon fluxes only the soft component of the neutrino spectrum of pion origin. In order to reconstruct the hard component of the spectrum, one must introduce information on the ratio of yields of K- and π-mesons from the target, as obtained from other experiments.

A combination of these two methods is used at CERN and IMEP. In other laboratories the determination of the neutrino spectrum is mainly based on data from measuring the meson yields.

In some experiments, in order to compensate for the lack of reliable information on the neutrino spectra,[38] use is made of normalization of the data to the number of quasielastic interactions and to isobar production, starting with the charge symmetry and the energy-independence of the quasielastic interaction cross section and the cross sections for isobar production at high energy in an isoscalar target:

$$\sigma(\nu_\mu + T \to \mu^- + N \text{ or } N^*) = \sigma(\bar{\nu}_\mu + T \to \mu^+ + N \text{ or } N^*) \approx \text{const}.$$

However, the number of such events is relatively small. In order to increase the statistical accuracy in normalizing the neutrino and antineutrino spectra (with the aim of extending into the region of higher energies, where the number of interactions is small, an attempt has also been made to include events with higher hadron masses in inelastic collisions.[39]

b) Electronic detectors

The low interaction cross sections of neutrinos at the present intensities and with the present method of producing neutrino beams require one to use massive targets, which must simultaneously fulfill the function of analyzing the interactions that occur.

Detectors based on spark chambers and scintillation counters are finding widespread application in experiments. Most recently, information on particle tracks (products of neutrino interactions is beginning to be obtained by using drift chambers. It is relatively simple to build electronic detectors of large mass and to optimize them for solving some limited group of problems. The restricted universality as compared with bubble chambers is compensated by the potentialities for considerably increasing the volume and weight of the detector and substantially reducing the resolving time. These factors substantially improve the background conditions and allow one to accumulate statistical material more rapidly.

We can subdivide the currently utilized electronic detectors into two groups, somewhat arbitrarily:

1. The target-analyzer is based on a hadron scintillation calorimeter. The particle-track devices serve to distinguish muons.

2. The target-analyzer is based on spark chambers. Scintillation counters arranged between them are auxiliary in nature, for providing a trigger or for time marking.

Most of the electronic detectors are supplemented by blocks made of ordinary or magnetized iron, solely for identifying, or else for identifying and determining the momentum of muons.

Methods of calorimetry of hadron energy are increasingly being used in the apparatus for studying neutrinos. In line with the fact that the dimensions of the region of the calorimeter in which ionization occurs depend only logarithmically ($\sim \ln E_H$) on the change in hadron energy, such instruments are very convenient for neutrino studies, where the energy spectrum of the beam is very broad. Employment of hadron calorimeters is associated with the fact that much interesting information does not depend on a knowledge of the detailed characteristics of individual hadrons. Thus, in inclusive processes with charged currents (CC) in which a muon and hadrons are produced in the final state, the kinematics of the interaction is completely determined if the total energy of the hadrons (E_H) and the magnitude (P_μ) and direction (θ_μ) of the momentum of the muon are measured since it is assumed that the direction of the neutrino is well known. The muonless interactions (NC) are also well identified, since the large sensitive volume of the detector amounts to active shielding of several nuclear interaction lengths from the external background.

Table II lists the electronic detectors with which experimental data have been obtained on the interaction of neutrinos and antineutrinos presented in this review.

Scintillation counters interleaved with iron filters,[46, 47] or large volumes of a liquid scintillator[42, 45] are used as hadron calorimeters.

The detailed calibration measurements for the detectors of the HPWF and CITF groups have shown a good linearity in the energy dependence and an improvement of resolution with increasing energy: $\Delta E_H/E_H \sim (E_H)^{-1/2}$. In pure scintillation calorimeters it amounts to (15–20)% in the energy range from several GeV up to ~100 GeV. In iron-plate detectors the resolution varies from ~40% to ~10% in the same energy range.

In detectors based on spark chambers the energy release is determined by counting the number of sparks.[48] According to the existing experimental data,[40, 41] these detectors possess analogous characteristics.

The momentum P_μ of the muons is measured by magnetic spectrometers, which amount to sets of magnetized iron disks or plates and spark chambers set up between them. Multiple scattering of the muons in the iron affects the accuracy of measurement in these systems. The accuracy depends on the value of the magnetic field (B) and the path traversed by the muon in the iron (L), and (neglecting the errors of measurement), it does not depend on the momentum:

$$\frac{\Delta p_\mu}{p_\mu} \approx 5.2 \cdot 10^{-2} (B \sqrt{L})^{-1}.$$

The resolution varies with the design of the detector, and as a rule it amounts to ~10% for energies below 10 GeV, and reaches ~20% for $p_\mu \sim 100$ GeV/c.

TABLE II. Electronic detectors of neutrino interactions.

Accelerator	Group	Experimental apparatus	Weight of target, T*	Physical problems	References
CERN	Aachen-Padua (AP)	Spark chambers with Al filters, muon identifier	50 (19)	$\nu_\mu e$, $(\nu\pi^0 N)$	40, 41
	CERN-Dortmund-Heidelberg-Saclay (CDHS)	Scintillators with magnetized Fe filters, drift chambers	1250 (900)	$\nu_\mu(\bar{\nu}_\mu)+N \to 2\mu+X$, inclusive CC	155
BNL	Harvard-Pennsylvania-Wisconsin (HPW)	Liquid scintillation modules, drift chambers	33	$\nu_\mu p \to \nu_\mu p$	48 (Fig. 7)
	Columbia-Illinois-Rockefeller (CIR)	Spark chambers with Al filters, scintillation counters	26 (8)	$\nu p \to \nu p$, $\nu N \to \nu\pi^0 N$, $\nu_\mu N \to \mu e + \ldots$	43
IHEP	ITEP-IHEP (IS)	Spark chambers with Fe filters, muon spectrometer	96 (34)	$\nu_\mu + N \to 2\mu + X$, inclusive CC	44 (Fig. 8)
FNAL	Harvard-Pennsylvania-Wisconsin-Fermilab (HPWF)	Liquid scintillator modules, spark chambers, muon spectrometer	60 (10–20)**	$\nu_\mu(\bar{\nu}_\mu)+N \to \to 2\mu+\ldots$, inclusive CC, inclusive NC	45, 157 (Fig. 9)
	Caltech-Fermilab (CITF)	Scintillators with Fe filters, spark chambers, muon spectrometer	160 (100)	$\nu_\mu(\bar{\nu}_\mu)+N \to 2\mu$, inclusive CC, inclusive NC	46 (Fig. 10)

Note: The physical analysis of the events is carried out for the target weight indicated in parenthesis.
Note: Depending on the physical problem.

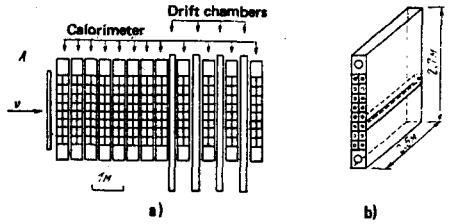

FIG. 7. Setup of the HPW group at BNL. a) side view; b) unit module.

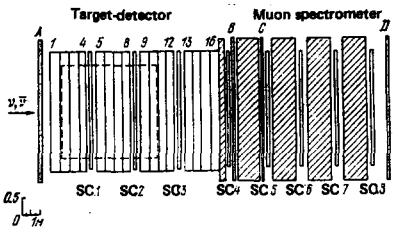

FIG. 9. Setup of the HPWF group at FNAL.

In processes that follow charged-current channels (*CC*), the energy of the interacting neutrino is determined simply as the sum $E_\nu = E_H + E_\mu$. One of the fundamental characteristics of a detector is its efficiency in determining various parameters of the interaction as a function of the neutrino energy. As an example, Fig. 11 shows for the CITF detector[46] the efficiency for events in which the muon passes through the magnet (solid line) and for all *CC* events with an identified muon (dotted curve).

c) Bubble chambers

The methodology of bubble chambers is currently widely used in neutrino experiments. This is explained, on the one hand, by the fact that the neutrino flux levels and small interaction cross sections allow bubble chambers to "digest" the full intensity of protons attainable in modern accelerators, and on the other hand, by the specific properties of bubble chambers as 4π-detectors that can analyze the separate reaction channels, including the visible modes of decay of strange particles.

Table III gives the characteristics of the large bubble chambers as neutrino detectors that are used in the laboratories of the United States (Argonne (ANL), Brookhaven (BNL), Batavia (FNAL)), CERN, and the USSR (Institute of High Energy Physics).[49-54] We see from this table that use has begun to be made in high energy neutrino experiments not only of chambers filled with heavy materials, but also of hydrogen bubble chambers, which offer an outstanding potential for analyzing neutrino-nucleon reactions under clean conditions. On the other hand, chambers filled with heavy materials or hydrogen chambers with added neon allow a faster accumulation of the statistics of events and a high efficiency of detecting electrons and γ-quanta (from 60% in the case of H_2 + 20% Ne to ~100% for Freon). The momenta of the charged particles (with an error in determining the spatial coordinates of 0.3–0.7 mm) are measured over the range 1–100 GeV/c with an accuracy of 1–10% for a track length up to two meters.

A certain difficulty in bubble chambers is presented by muon identification and by the individual determination of the energy of the neutrino in each particular event.

The method of distinguishing the muon in pure hydrogen chambers is based either on the kinematics of neutrino reactions[55] (i.e., distinguishing the muon by the value of the transverse momentum $p_\perp$, which considerably exceeds the mean transverse momentum of the hadrons at high neutrino energies), or on using an external muon identifier. Figure 12 gives an example of such an instrument as used in experiments with the 15-foot bubble chamber of FNAL.[56] It consists of a system of proportional chambers that cover a relatively large solid angle and a hadron absorber of a thickness of 3–4 nuclear interaction lengths situated between the volume of the bubble chamber and the planes of the proportional chambers. For more reliable muon identification in recent experiments, people are beginning to employ a second plane of proportional chambers situated beyond an additional absorber. The overall efficiency of the external muon identifier amounts to about 80%. One of the defects of such apparatus is the low efficiency for large y and a rather considerable threshold (3 GeV). Unquestionably it is an irreplaceable means for identifying rare events.

In bubble chambers one determines the total neutrino energy E_ν by measuring the momenta of the detected charged particles, with correction for the energy of the neutral unrecorded hadrons or γ-quanta. Thus, in an experiment of the FIMS (FNAL-Institute of Theoretical and Experimental Physics-Michigan-Serpukhov) group[114] this correction was introduced by using the correlation between the longitudinal component of the visible hadron momentum p_x^h and the total hadron energy ν_H (Fig. 13) which follows from $p_\perp$ balance. In order to allow for this correction, one can also use the statistical method,[57] in which one can treat not each event individually, but rather the distributions over the measured kinematical variable taking into account the known distribution function for the undetected component. The reso-

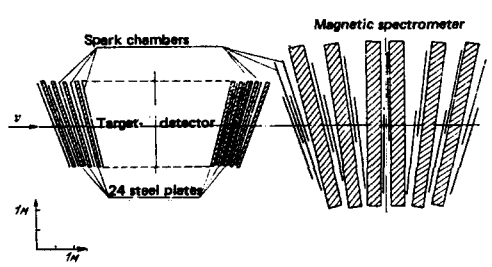

FIG. 8. Setup of the IS group at IHEP.

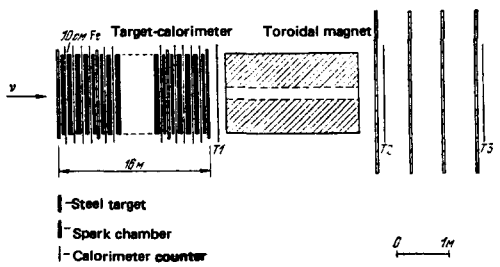

FIG. 10. Setup of the CITF group at FNAL.

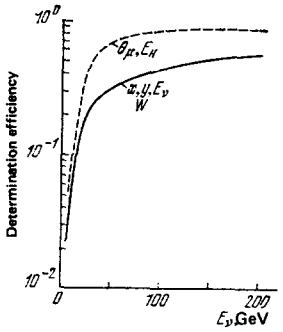

FIG. 11. Efficiency of determining the kinematic parameters for the CITF setup.

lution in E_ν usually amounts to 8–15%, depending on the material used in filling the bubble chamber.

Owing to the lack of time selection in bubble chambers, the hadron background presents considerable difficulty. Thus, for the broad neutrino spectrum of FNAL, this background is most substantial in the range $E_\nu < 10$ GeV. This complicates the analysis of events involving neutral currents. For energies above 10 GeV, it amounts to ~1%.

3. TOTAL CROSS SECTIONS

The most general, characteristic properties of weak processes at high energies can be understood from studies involving measurement of the total cross sections for the interaction of neutrinos with nucleons. In this section we present data both for processes involving charged currents ($\sigma_C^\nu, \sigma_C^{\bar\nu}$):

$$\nu_\mu(\bar\nu_\mu) + N \to \mu^-(\mu^+) + \text{hadrons}, \qquad (3.1)$$

and for processes involving neutral currents ($\sigma_N^\nu, \sigma_N^{\bar\nu}$):

$$\nu_\mu(\bar\nu_\mu) + N \to \nu_\mu(\nu_\mu) + \text{hadrons}, \qquad (3.2)$$

At present the process (3.1) has been studied more fully. Hence it is precisely these data, together with the differential scaling distributions, that give important information on the local nature of the weak interactions and the validity of the scaling hypothesis and the quark-parton model of the nucleon. The fundamental results have so far been obtained with nuclei having an equal or approximately equal proton-neutron ratio, i.e., with isotopically scalar targets.

TABLE III.

Bubble chamber	Filling	Abbreviation of the group*	Working volume, m^3	Weight T	L_0, cm	H, kgauss	Beam
"Gargamelle", CERN[52]	CF_3Br	GGM	5—6	7—9		20	$\nu, \bar\nu$
12', ANL (USA)[53]	H_2, D_2	ANL	16	1—2		20	ν
7', BNL (USA)[54]	H_2, D_2	BNL	6	0.4		25	ν
15', FNAL (USA)[49]	H_2	FM	20	1.3		21. 30	ν
	H_2	AMP	20	1.3		21. 30	$\bar\nu$
	H_2+Ne (20%)	BCHW	20	7		30	ν
	H_2+Ne (20%)	FIMS	20	7		30	$\bar\nu$
	H_2+Ne (64%)	CB	20	22		30	ν
	H_2+Ne (64%)	BS	20	22		30	$\bar\nu$
SKAT, IHEP (USSR)[50]	CF_3Br	SKAT	4.5	7		20. 25	ν
BEBC CERN[51]	H_2, D_2, Ne	BEBC	20—25	—		35	$\nu, \bar\nu$

Note. GGM = Aachen-Brussels-CERN-École Polytechnique-Orsay-London; FM = FNAL-University of Michigan (with participation of physicists from IHEP and ITEP); AMP = ANL-Mellon-Purdue; BCHW = Berkeley-CERN-Hawaii-Wisconsin; FIMS = FNAL-ITEP-University of Michigan-IHEP (Serpukhov); CB = Columbia University-BNL; BS = Berkeley-Seattle.

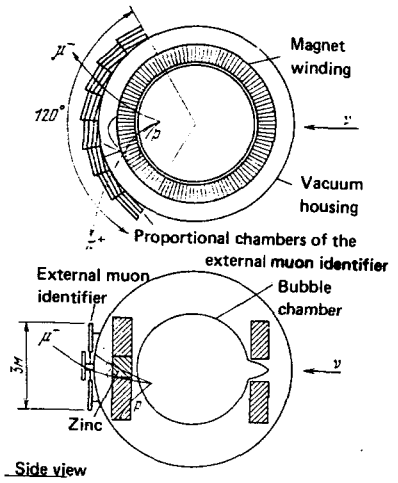

FIG. 12. The FNAL 15-foot bubble chamber with external muon identifier.

It is considerably more complicated to detect the process (3.2), and this has been the fundamental reason for the almost ten-year lag in its discovery (semilepton neutral currents were first detected in an experiment at CERN in the bubble chamber Gargamelle in 1973[58,83]). Currently the experimental data on the ratios $R^\nu = \sigma_N^\nu / \sigma_C^\nu$ and $R^{\bar\nu} = \sigma_N^{\bar\nu}/\sigma_C^{\bar\nu}$ are of great interest for testing the consequences of the gauge-invariant theory and establishing the structure of the weak neutral current.

In this section we shall also present the results of the first measurements of cross sections involving the electron neutrino, which are of interest in connection with the problem of μ-e universality at high energies.

a) Total cross sections for processes involving charged currents

In the scaling hypothesis the cross section for inelastic processes is expressed in terms of the energy-independent structure functions of the nucleon and the scaling variables x, y, and E_ν as follows:[23,59]

$$\frac{d^2\sigma_c^{\nu,\bar\nu}}{dx\,dy} = \sigma_0\left[(1-y)F_2(x) + \frac{y^2}{2}2xF_1(x) \pm y\left(1-\frac{y}{2}\right)xF_3(x)\right], \qquad (3.3)$$

where F_1, F_2, and F_3 are the structure functions for axial-vector (A), vector (V), and interference (VA) interactions; and $\sigma_0 = G^2 m_N E_\nu/\pi$. Integration with respect to x and y over the interval 0–1 gives

$$\sigma_c^{\nu,\bar{\nu}} = \sigma_0 \frac{3 + A \pm 2B}{6} \int_0^1 F_2(x)\, dx, \tag{3.4}$$

where we have

$$A = \int_0^1 2xF_1(x)\, dx \Big/ \int_0^1 F_2(x)\, dx, \tag{3.5}$$

$$B = \int_0^1 xF_3(x)\, dx \Big/ \int_0^1 F_2(x)\, dx. \tag{3.6}$$

Hence the ratio of the total cross sections

$$R_c = \frac{\sigma_c^{\bar{\nu}}}{\sigma_c^{\nu}} = \frac{3 + A - 2B}{3 + A + 2B}, \tag{3.7}$$

does not depend on the energy. In addition, if we identify the parton with a quark of half-integral spin, then $2xF_1 = F_2$.[60] This gives $A = 1$. The value of the parameter B, which is defined in this model in terms of the effective density of quarks $q(x)$ and of antiquarks $\bar{q}(x)$ in the nucleon, is

$$B = 1 - 2\frac{\int \bar{q}(x)\, dx}{\int (q(x) + \bar{q}(x))\, dx} = 1 - 2\frac{\bar{Q}}{Q + \bar{Q}}. \tag{3.8}$$

In the first approximation we can take it to be unity. Hence R_c has a value $\approx 1/3$ and does not depend on the energy.[2)]

The most accurate measurements of the total cross sections in the energy range 1–10 GeV have been performed at CERN with the Gargamelle chamber filled with Freon.[61,62] These results are the cross sections per "nucleon" of Freon as based on the statistics of 2500 νN and 950 $\bar{\nu}N$ events shown in Fig. 14. The indicated errors are only statistical. The possible systematic errors due to uncertainties in the normalizations of the neutrino flux and in the corrections for event selection and energy resolution amount to about 10%.

This same diagram shows the data of the ANL group,[63] which were obtained in hydrogen and deuterium in a bubble chamber and were averaged per "nucleon" over the protons and neutrons.

In this energy range (1–10 GeV) the total cross sections are well described by a linear relation that corresponds to the scaling behavior of (3.3):

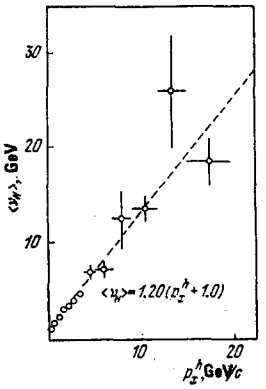

FIG. 13. Dependence of the mean hadron energy $\langle \nu_H \rangle$ on the longitudinal component of the visible hadron momentum p_x^h.

$$\sigma_c^{\nu} = \alpha_\nu E_\nu = (0.74 \pm 0.02) \cdot 10^{-38} E_\nu \text{ cm}^2,$$

$$\sigma_c^{\bar{\nu}} = \alpha_{\bar{\nu}} E_{\bar{\nu}} = (0.28 \pm 0.01) \cdot 10^{-38} E_{\bar{\nu}} \text{ cm}^2.$$

The first experimental results on absolute measurements of total cross sections at high energies have been obtained by the CITF group[64] at Batavia. The cross sections for the two energies $E_{\nu,\bar{\nu}} = 38 \pm 14$ GeV and $E_{\nu,\bar{\nu}} \approx 105 \pm 21$ GeV are also shown in Fig. 14. They satisfy the values of the parameters α shown in this diagram with an uncertainty of about 20%. The first results of the HPWF group[65] also fully agreed with the data obtained at low energies.

New experimental results on the measurement of the total cross sections have recently been obtained by the CITF groups[154] (12 thousand νN and 6 thousand $\bar{\nu}N$ interactions) and in the BEBC bubble chamber at CERN[153] (520 νN and 250 $\bar{\nu}N$ interactions). A distinctive feature of this first experiment with the BEBC chamber, which was performed with a monochromatic beam in a Ne-H mixture (58 atom% Ne) is that the cross-sections were normalized by performing good measurements in the channel of the absolute flux of muons and of their angular distribution by using counters and photoemulsions.

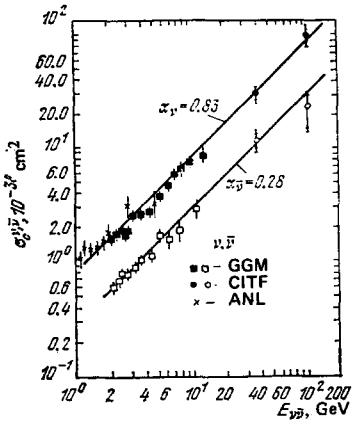

FIG. 14. Energy-dependence of the total interaction cross sections of neutrinos and antineutrinos with nucleons $\sigma_c^{\nu,\bar{\nu}}$.

[2)] More exactly, for an isoscalar target the 3-quark model gives the following expressions for the cross-sections in terms of the distribution functions of the quarks:

$$\frac{d\sigma^{\nu N}}{dx\, dy} = x[(u+d)\cos^2\theta_C + 2\sin^2\theta_C s + (\bar{d}+\bar{u})(1-y)^2],$$

$$\frac{d\sigma^{\bar{\nu}N}}{dx\, dy} = x[(u+d)(1-y)^2 + \cos^2\theta_C(\bar{u}+\bar{d}) + 2\sin^2\theta_C \bar{s}].$$

Hence, when we neglect antiquarks, $R_c \approx 1/3\cos^2\theta_C \approx 0.35$.

In an almost identical energy range (40–200 GeV), the two groups found the following slope parameters:

$\alpha_\nu = 0.59 \pm 0.03$. $\alpha_{\bar\nu} = 0.27 \pm 0.02$ (BEBC),
$\alpha_\nu = 0.60 \pm 0.06$, $\alpha_{\bar\nu} = 0.29 \pm 0.03$ (CITF).

The table gives the more detailed data of the BEBC group:

E_ν ($\bar\nu$), GeV	20—60	60—100	100—150	150—200
α_ν	0.67±0.06	0.56±0.05	0.61±0.05	0.51±0.05
$\alpha_{\bar\nu}$	0.28±0.03	0.25±0.03	0.32±0.04	

The BEBC data do not include systematic errors, which amount to 8% according to estimates of the authors.

Although, as the authors note, the variations in the cross sections in the energy range 40–200 GeV lie within the limits of the experimental uncertainties, yet if we compare the mean values of the slope parameters in the two regions 1–10 and 40–200 GeV, we can note a certain reduction in the rate of increase of the cross-sections for the νN interactions. We can interpret this result within the framework of deviation from Bjorken scaling. It is difficult at present to carry out a more exact analysis using these measurements of the total cross sections, if only because the deep inelastic scattering should not include elastic or almost elastic interactions having $q^2 \ll 1$ GeV, whereas the data at small energies do include them. One of the conclusions drawn by the authors of Ref. 154 is that the existing measurements of the energy trend of the total cross sections allow one to establish a mass limit for the intermediate W-boson, which proves to be $m_W > 30$ GeV/c^2.

In principle, one can draw more definite conclusions from measurements of the values R_c of the ratios of the cross-sections for $\bar\nu N$ and νN interactions, which are less subject to systematic errors and less sensitive to the criteria of selection of inelastic events. Figure 15 presents the results of all the experiments performed up to now.

From the data of CERN (Gargamelle),[61] the value $R_c = 0.37 \pm 0.02$ for $2 < E_{\nu,\bar\nu} < 14$ GeV exhibits no energy dependence. This corresponds to the simple quark model (dotted line in Fig. 15). Later, in 1976, the HPWF group[66] performed measurements that showed that R_c increases rather sharply with energy, starting at an energy of 40 GeV (Fig. 15).

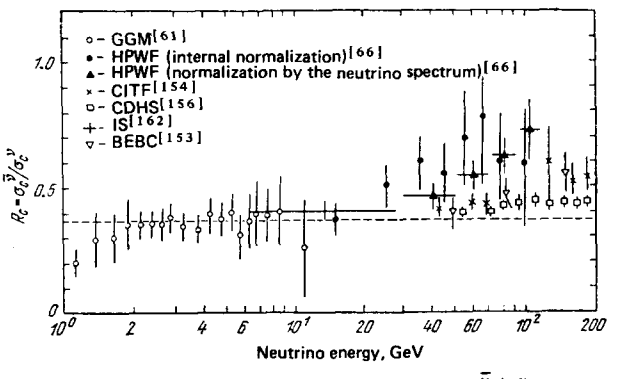

FIG. 15. Energy-dependence of the ratio $R_c = \sigma_c^{\bar\nu}/\sigma_c^{\nu}$.

In this experiment the data were obtained in two ways. In a beam with quadrupole focusing and a natural mixture of ν and $\bar\nu$ 2900 neutrino interaction events and 570 antineutrino events were obtained. In this case calculated information on the spectra was used. In the second case more abundant statistics (4994 neutrino and 2904 antineutrino interactions) were used, including also exposures in ν and $\bar\nu$ beams obtained using a horn. An attempt was made to normalize by an internal method by distinguishing quasielastic interactions, isobar production, and inelastic events with a small mass W of recoil of the hadron system.[39] As can be seen from Fig. 15, the two methods gave concordant results.

However, recent new measurements at CERN,[156, 153] IHEP,[162], and FNAL,[154] the results of which are also shown in Fig. 15, did not reveal such sharp changes in the ratio R_c in the energy range 6–200 GeV.

As can be seen from Fig. 15, the results of the already discussed experiments of the BEBC[153] and CITF[154] groups agree with one another, and indicate a slow rise in R_c to the level 0.5–0.55 at an energy of 200 GeV. The preliminary data of the experiment at CERN with the best statistics,[156] which was performed using a new electronic detector (36 thousand νN and 12 thousand $\bar\nu N$ interactions), show that the ratio R_c is practically constant at the level of 0.43 over the energy range 40–200 GeV.

In summarizing the overall situation in the measurements of total cross sections for charged currents we can draw the following conclusion.

In the broad energy range 2–200 GeV the total cross sections increase linearly or almost linearly with increasing energy, both for νN and for $\bar\nu N$ interactions. There is an indication of an increase in the ratio $R_c = \sigma_c^{\bar\nu}/\sigma_c^{\nu}$ with the energy in the range 10–200 GeV by 20–30%, which is associated with a decline in the rate of increase of the cross sections for νN interactions.

This behavior of the energy-dependence of the total cross sections agrees with the overall pattern of deviation from exact scaling behavior of the structure functions in deep inelastic lepton-nucleon interactions, as will be discussed in section V of this review.

b) Ratio of the total cross sections for the interaction with neutrons and protons

Measurements of the ratio of the total cross sections for interaction with neutrons and protons have recently been performed in deuterium in bubble chamber experiments by the ANL and BNL groups. Table IV gives these results together with the data obtained at CERN with heavy-liquid bubble chambers.

The ratio $\sigma_c^{\nu n}/\sigma_c^{\nu p}$ obtained from the quark model[103, 106] (with account taken of the $q\bar q$ "sea") is 1.8–2.1, and this refers to the deep inelastic energy region, which is higher than the mean energies of the cited experiments.

TABLE IV.

Experiment	Energy, GeV	$\sigma_c^{\nu n}/\sigma_c^{\nu p}$
ANL (H_2, D_2)[68]	2—6	1.40±0.31
BNL (H_2, D_2)[69]	1—10	1.4±0.14
	$\nu_H > 0.8$	1.04±0.16
CERN[70] "Gargamelle" (C_3H_8)	1—10	2.1±0.3
CERN[71] 1.2 m (C_3H_8)	1—10	1.8±0.3

There are no published data for the ratio $(\sigma_c^{\bar{\nu}n}/\sigma_c^{\bar{\nu}p})$ except for a preliminary estimate obtained by the FIMS group in an experiment with the 15-foot bubble chamber in a neon-hydrogen mixture for the range $E_{\bar{\nu}} = 10$–100 GeV,[72] which was 1.98 ± 0.30.

c) Total cross sections for inclusive semilepton reactions involving neutral currents

Measurements of the total cross sections for the process (3.2) involving neutral currents (more correctly, of the ratios R^{ν} and $R^{\bar{\nu}}$) have been performed in the last several years by the GGM (CERN),[58,73], CITF,[74] and HPWF (Batavia)[75] groups. We present below the most recent results obtained in 1976 (Table V). Columns 4 and 3 of Table V indicate the corresponding numbers of *NC*-and *CC*-events (neutral and charged currents) after introduction of all the experimental corrections. The last column gives the ratios $R^{\nu,\bar{\nu}}_{\text{meas}}$ found for identical hadron-energy cutoffs E_H, both for *NC*- and for *CC*-events. In order to obtain from $R^{\nu,\bar{\nu}}_{\text{meas}}$ the true values of $R^{\nu,\bar{\nu}}$ or $\sigma_N^{\bar{\nu}}/\sigma_N^{\nu}$, one must introduce additional corrections involving failure to detect a fraction of the events owing to the application of a cutoff for E_H. In view of the difference in y distributions for ν and $\bar{\nu}$, these corrections differ substantially for R^{ν} and $R^{\bar{\nu}}$, and one can introduce them only by assuming a particular form of the interaction involving a neutral current, i.e., they are model-dependent.

It is most convenient to represent all the data in a general form by assuming that the weak neutral currents are a linear combination of only V and A variants, that the Bjorken scaling is valid, and that the interaction occurs between point objects of half-integral spin. Then we can write:

$$\left.\begin{aligned}\frac{d\sigma_N^{\nu}}{dy} &= \frac{G^2 m_N E_{\nu}}{\pi}[A_L + A_R(1-y)^2],\\ \frac{d\sigma_N^{\bar{\nu}}}{dy} &= \frac{G^2 m_N E_{\bar{\nu}}}{\pi}[A_L(1-y)^2 + A_R],\end{aligned}\right\} \tag{3.9}$$

where A_L and A_R can be treated as coupling constants of negative and positive helicity, respectively.

TABLE V.

Experiment	Beam $\langle E_{\nu,\bar{\nu}}\rangle$, GeV	Number of *CC* events	Number of *NC* events	Cutoff energy E_H for hadrons	$R^{\nu,\bar{\nu}}_{\text{meas}}$
GGM[13]	$\langle 2.5\rangle$ ν	631	159	>1	0.25±0.04
	$\langle 2.0\rangle$ $\bar{\nu}$	235	131		0.56±0.09
HPWF[75]	$\langle 85\rangle$ ν	1042	300	>4	0.29±0.04
	$\langle 41\rangle$ $\bar{\nu}$	198	69		⩽0.39±0.10
CITF[74]	$\langle 52\rangle$, $\langle 146\rangle$ ν	1918±57	457±41	>12	0.24±0.02
	$\bar{\nu}$	274±26	94±24		0.34±0.09

TABLE VI.

Experiment	$P = A_R/(A_R + A_L)$	R^{ν}	$R^{\bar{\nu}}$	$\sigma_N^{\bar{\nu}}/\sigma_N^{\nu}$	$\sin^2\theta_W$
"Gargamelle"	0.25±0.07	0.25±0.04	0.39±0.06	0.58±0,17	0.33±0.05
CITF	0.36±0.09	0.25±0.04	0.35±0.09	0.75±0,14	0.33±0.05
HPWF	0.15±0.10	0.29±0.04	0.31±0.09	0.48±0,20	~0.29

Table VI gives the ratios $P = A_R/(A_R + A_L)$ for all three experiments, as well as the corrected values of R^{ν}, $R^{\bar{\nu}}$, and $\sigma_N^{\bar{\nu}}/\sigma_N^{\nu}$. Theoretically the ratio P should be close to 0.05 (with account for the content of antiquarks) for the pure V-A variant, or to 0.5 for the V or A variant, or to 1 for the $V+A$ variant. We also note that using an analogous treatment the GGM group obtained the value $P = 0.05 \pm 0.05$ for events involving charged currents. One can conclude from comparing these values and the data given in Table V that the $V+A$ variant of the interaction is ruled out. The expected values of P for the V and A variants individually differ on the average from the experimental values by more than three standard deviations, whereas the pure $V-A$ variant also does not agree very well with experiment.

The CITF group has fitted its data to a three-term formula instead of (3.9), i.e., they tried to determine the contribution of the P and S variants. They obtained the value $A_{P,S} = -0.2 \pm 0.1$, i.e., different from zero by only two standard deviations and with a negative sign. In the Weinberg-Salam model using a three-quark scheme and neglecting the interaction with the quarks of the "sea", we have the following relationships:[76]

$$\left.\begin{aligned}R^{\nu} &= \frac{1}{2} - \sin^2\theta_W + \frac{20}{27}\sin^4\theta_W,\\ R^{\bar{\nu}} &= \frac{1}{2} - \sin^2\theta_W + \frac{20}{9}\sin^4\theta_W,\\ \frac{\sigma_N^{\bar{\nu}}}{\sigma_N^{\nu}} &= \frac{1}{3}\frac{R^{\bar{\nu}}}{R^{\nu}}.\end{aligned}\right\} \tag{3.10}$$

The curve in Fig. 16 was obtained in accordance with the formulas of (3.10). The same diagram shows the experimental, corrected values of R^{ν} and $R^{\bar{\nu}}$. As can be seen from the values given in Table VI, the data (the latter are calculated taking into account the contribution from the quarks of the "sea", which is 5%) fit the value $\sin^2\theta_W = 0.33$.

Thus we can draw the following conclusions from the experimental data on inclusive semilepton reactions involving a neutral current in neutrino experiments.

1. The ratios of the cross sections for muonless reactions to those for reactions involving charged currents amount to 0.26 ± 0.05 for νN and 0.35 ± 0.09 for $\bar{\nu}N$ interactions for combinations of the V and A variants of the interaction, and the energy-dependence of the cross section σ_N does not contradict a linear growth within the limits of experimental error.

2. The $V+A$ form of interactions is ruled out for neutral currents, as well as the V and A variants individually. The experimental data agree best with a mixed $(V - 0.8A)$ variant of the interactions. This means that the neutral currents, just like the charged currents, contain a considerable component that does not conserve

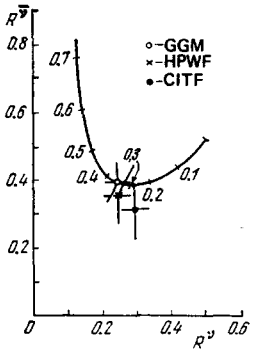

FIG. 16. Experimental values of R^{ν} and $R^{\bar\nu}$. Theoretical curve—calculated by Eq. (3.10).

parity.

3. The data on the semi-inclusive reactions involving neutral currents agree with the value of the Weinberg angle $\sin^2\theta_W = 0.33 \pm 0.05$.

4. The further study of neutral currents will require experiments with monochromatic beams and under pure conditions (hydrogen, deuterium).

d) μ–e universality

On the basis of the statistics of 191 $\nu_e N$ interactions and 84 $\bar\nu_e N$ interactions, the GGM group has determined in a Freon bubble chamber[61, 160] the total cross sections for an electron neutrino incident on a nucleon:

$$\left.\begin{aligned} &\sigma_c^{\nu_e} = (0.88 \pm 0.08)\, E_{\nu_e} \cdot 10^{-38}\,\text{cm}^2/\text{nucleon}, \quad \frac{\sigma_c^{\nu_e}}{\sigma_c^{\nu_\mu}} = 1.11 \pm 0.15,\\ &\sigma_c^{\bar\nu_e} = (0.33 \pm 0.04)\, E_{\bar\nu_e} \cdot 10^{-38}\,\text{cm}^2/\text{nucleon}, \quad \frac{\sigma_c^{\bar\nu_e}}{\sigma_c^{\bar\nu_\mu}} = 1.10 \pm 0.17,\\ &\frac{\sigma_c^{\bar\nu_e}}{\sigma_c^{\nu_e}} = 0.38 \pm 0.06. \end{aligned}\right\} \quad (3.11)$$

As can be seen by comparing the data of (3.11) with those for the muon neutrino, μ–e universality holds to a first approximation in charged currents at high energies.

There are as yet no data whatsoever on the interaction of electron neutrinos in neutral currents.

4. ELASTIC AND SINGLE-PION PROCESSES

a) Quasielastic and elastic scattering by nucleons

Quasielastic (qe) scattering of neutrinos and antineutrinos by nucleons

$$\nu_\mu + n \to \mu^- + p, \quad (4.1)$$
$$\bar\nu_\mu + p \to \mu^+ + n \quad (4.2)$$

is usually described under the traditional assumptions of invariance with respect to time reversal, absence of weak currents of the second type,[77] and with neglect of the induced pseudoscalar[78] interaction. Under these assumptions we have

$$\frac{\sigma_{xy}^{\nu(\bar\nu)}}{dq^2} = \frac{G^2}{4\pi}\left\{(F_V \pm F_A)^2 + (1-y)^2(F_V \mp F_A)^2 - \frac{q^2}{2E_\nu^2}(F_V^2 - F_A^2) + 2yF_M\left[(1-y)\frac{E_\nu}{2m_N}F_M + y(F_M + F_V \mp F_A) \pm 2F_A\right]\right\},$$

where we have set $F_M \approx (\mu_p - \mu_n)F_V$, $F_{V,A} = F_{V,A}(0)/(1 \mp q^2/M_{V,A}^2)^2$, where μ_n and μ_p are the magnetic moments of the nucleons, $F_V(0) = 1$, and $F_A(0) = 1.23$ from the β-decay of the neutron ($q^2 = 0$), i.e., the scattering is fully determined by the two parameters M_V and M_A. If in addition we extend the hypothesis of conserved vector current (CVC) to neutrino interactions, we get $M_V = 0.84$ GeV/c^2 from electron-scattering experiments.

The ANL group[79] has obtained the most recent results on quasielastic scattering in a neutrino beam in a 12-foot bubble chamber filled with deuterium.

They performed the analysis by two methods for determining M_A: fitting the parameter M_A to the $\sigma_{qe}(E_\nu)$ relationship and fitting it to the $d\sigma_{qe}/dq^2$ relationship. The first method hinges on knowing the energy spectrum of the neutrinos, and it directly includes errors due to its uncertainty, while the second method does not depend on knowing the energy spectrum.

The result obtained is: 1) $M_A^\nu = 0.98^{+0.13}_{-0.14}$ GeV/c^2, 2) $M_A^\nu = 0.84^{+0.12}_{-0.10}$ GeV/c^2. The averaged value is $M_A = 0.89 \pm 0.08$. Simultaneous determination of the two parameters M_V and M_A gives: $M_V^\nu = 0.92^{+0.05}_{-0.11}$ GeV/c^2, $M_A^\nu = 0.75^{+0.21}_{-0.10}$ GeV/c^2.

Data on quasielastic scattering of neutrinos and antineutrinos have been obtained at CERN using the Gargamelle chamber filled with Freon.[61, 80] An analogous analysis by the two methods gives:

1) $M_A^\nu = 0.96 \pm 0.10$. $M_A^{\bar\nu} = 0.7 \pm 0.2$,
2) $M_A^\nu = 1.0 \pm 0.1$. $M_A^{\bar\nu} = 0.91 \pm 0.12$.

The value averaged over these data is $M_A = 0.94 \pm 0.06$ GeV/c^2.

The most recent results on electroproduction of pions[81] give the value $M_A = 0.96 \pm 0.03$, which agrees well with the neutrino data.

Figure 17 shows the dependence of the quasielastic scattering cross sections on the energy $E_{\nu,\bar\nu}$.

In view of its simplicity, the elastic scattering of neutrinos and antineutrinos

$$\text{a)}\ \nu_\mu + p \to \nu_\mu + p, \quad \text{b)}\ \nu_\mu + n \to \nu_\mu + n, \quad (4.3)$$
$$\text{a)}\ \bar\nu_\mu + p \to \bar\nu_\mu + p, \quad \text{b)}\ \bar\nu_\mu + n \to \bar\nu_\mu + n, \quad (4.4)$$

is of great interest for studying neutral currents.

Since they follow an analogous phenomenology, the differential cross-sections for the reactions (4.3a) and (4.4b) can be written in the same form as for quasielastic scattering with the replacement of the corresponding form factors: $F_A \to F_A^0$, $F_V \to F_V^0$, and $F_M \to F_M^0$.

The Salam-Weinberg model establishes the relationship:[82, 83]

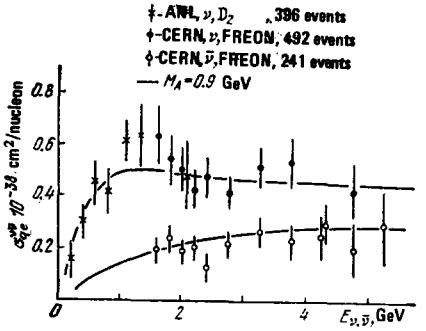

FIG. 17. Energy-dependence of the quasielastic scattering cross-section $\sigma_{qe}^{\nu\nu}$ for neutrinos and antineutrinos.

$$F_V^0 = \frac{1}{2} F_V - 2\sin^2\theta_W \cdot F^{em},$$
$$F_A^0 = \frac{1}{2} F_A, \qquad (4.5)$$

and again $d\sigma^0/dq^2$ remains a function of the sole parameter of the model: $\sin^2\theta_W$.

Two groups have recently observed elastic scattering with the BNL accelerator.

The Columbia-Illinois-Rockefeller (CIR) group[84] used for this purpose a setup with spark chambers, and found

$$R_{\text{elast}}^{\nu\mu} = \frac{\sigma(\nu_\mu + p \to \nu_\mu + p)}{\sigma(\nu_\mu + n \to \mu^- + p)} = 0.23 \pm 0.09.$$

An experiment by the Harvard-Pennsylvania-Wisconsin (HPW) group[85,86] studied scattering by using a scintillation calorimeter. At a background level of 30–40% they observed respectively 150 and 40 events of the reactions (4.3) and (4.4). They found that $R_{\text{elast}}^{\nu\mu} = 0.17 \pm 0.05$ and $R_{\text{elast}}^{\bar\nu\mu} = 0.2 \pm 0.1$ in the range of q^2 from 0.3 to 0.9 (Gev/c^2). We should note, however, that we must introduce a model-dependent correction into these values that takes into account the contribution of the reactions (4.3b) and (4.4b). If we estimate the contribution of the $\nu n - \nu n$ reactions according to the Weinberg model, then the ratios acquire the following values:

$$R_{\text{elast}}^{\nu\mu} = 0.10 \pm 0.03,$$

$$R_{\text{elast}}^{\bar\nu\mu} = 0.10 \pm 0.05.$$

Figure 18 shows the distribution of elastic events with respect to q^2. We can also see from Fig. 18 the agreement between the differential distributions with respect to q^2 for elastic and quasielastic events.

The data of this experiment imply the following ratio:

$$\frac{\sigma(\bar\nu_\mu + p \to \bar\nu_\mu + p)}{\sigma(\nu_\mu + p \to \nu_\mu + p)} = 0.4 \pm 0.2.$$

If the structure of the neutral current were purely vectorial, then this ratio would be unity.

Thus, just like the total cross sections for the neutral-current processes, already the first observations of elastic reactions imply that there is a substantial admixture of the axial-vector variant, which does not conserve parity.

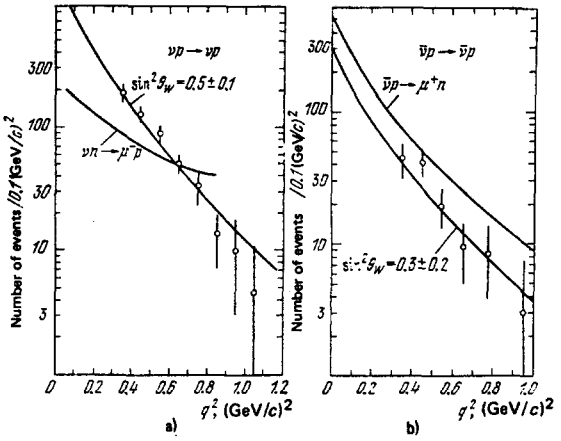

FIG. 18. The q^2-dependence of elastic and quasielastic scattering (data of the HPW group) for νN interaction (a) and $\bar\nu N$ interaction (b).

b) Elastic scattering of neutrinos by electrons

Processes of elastic scattering of neutrinos by electrons have attracted attention since the time of establishment of the universal Fermi interaction, in line with the fact that they are among the few weak processes in which only leptons participate. However, because of the experimental difficulties and the small cross sections (which are due to the low energy in the center-of-mass system of the electron and the neutrino), results have been obtained only recently.

The following reactions are possible:

$$\nu_\mu + e^- \to \nu_\mu + e^-, \qquad (4.6)$$
$$\bar\nu_\mu + e^- \to \bar\nu_\mu + e^-, \qquad (4.7)$$
$$\nu_e + e^- \to \nu_e + e^-, \qquad (4.8)$$
$$\bar\nu_e + e^- \to \bar\nu_e + e^-. \qquad (4.9)$$

The first two reactions can occur only via a neutral-current mechanism, whereas the latter two should occur both via charged and neutral currents. Figure 19 gives the expected relative values of the cross-sections as functions of $\sin^2\theta_W$.

The first observation of the antineutrino-scattering process of (4.7) was made in a CERN experiment using the Gargamelle chamber,[87] in which three events were

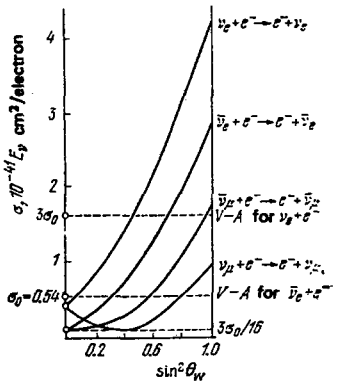

FIG. 19. Theoretical dependence of the cross-sections for the scattering of neutrinos and antineutrinos by an electron on $\sin^2\theta_W$).

observed in 1.3 million exposures ($4.7\times10^{18}p$ on target). The kinematics of the reaction (4.7) is such that under the conditions of the given experiment in order to minimize the background (Compton electrons, asymmetric e^+e^- pairs, the process $\nu_e+n\to e^-+p$ with an invisible recoil proton, as well as processes (4.8) and (4.9) it was possible to employ the criteria $\theta_e<5^\circ$, and $0.3<E_e<2$ GeV without large losses of the sought reaction. The total background estimated by the authors amounted to 0.44 ± 0.13 events.

They interpreted the data under the assumption that the neutral lepton current is an arbitrary linear combination of the V and A forms of interaction:[88]

$$l_\mu=\bar\nu\gamma_\mu(1+\gamma_5)\,\nu+e\gamma_\mu(G_V+G_A\gamma_5)\,e. \tag{4.10}$$

In this case the differential cross-section for the reaction (4.7) can be written in the following form:

$$\frac{d\sigma}{dy}=\frac{G^2m_eE_{\bar\nu}}{2\pi}[(G_V+G_A)^2(1-y)^2+(G_V-G_A)^2], \tag{4.11}$$

where the constants have been defined so that $G_V/G_A=+1$ for a pure $V-A$ current, and $y=E_e/E_{\bar\nu}$.

In calculating the scattering cross sections they took into account the efficiency of identification of electrons and the background level.

They found within the framework of the V,A-theory that

$$\sigma(\nu_\mu e^-)=0.10^{+0.21}_{-0.09}\cdot10^{-41}E_{\bar\nu}\ (\text{GeV})\text{cm}^2/\text{electron}.$$

where the errors correspond to the 90% confidence level. In the Weinberg-Salam model the constants G_V and G_A are defined as follows:

$$G_V=-\frac{1}{2}+2\sin^2\theta_W,\quad G_A=-\frac{1}{2}. \tag{4.12}$$

Then the result of (4.12) implies that $\sin^2\theta_W<0.4$ at the 90% confidence level.

A search was made for the reaction (4.6) in a neutrino exposure but owing to the higher background only a bound for the cross section was established:

$$\sigma(\nu_\mu e^-)<0.34\cdot10^{-41}E_\nu(\text{GeV})\text{cm}^2/\text{electron}.$$

Upon combining this result with the preceding one, the authors found that

$$0.1<\sin^2\theta_W<0.4.$$

Another experiment to study the processes (4.6) and (4.7) has recently been performed at CERN by the Aachen-Padua (AP) group[89] using an electronic detector. In this experiment they observed 25 candidates for the reaction (4.6) and 19 candidates for (4.7) at an appreciable background level.

They obtained the following cross sections and estimates:

$$\sigma(\nu_\mu+e^-)=(1.1\pm0.7)\,E_\nu\ (\text{GeV})\cdot10^{-42}\ \text{cm}^2/\text{nucleon},$$
$$\sigma(\bar\nu_\mu+e^-)=(2.4\pm1.1)\,E_{\bar\nu}\ (\text{GeV})\cdot10^{-42}\ \text{cm}^2/\text{nucleon},$$
$$\frac{\sigma_{\bar\nu}}{\sigma_\nu}=2.2\pm1.3;\quad \sin^2\theta_W=0.33\pm0.07.$$

These values agree satisfactorily with the data of the Gargamelle group.

The elastic scattering of electron antineutrinos (4.9) has been measured recently by Reines' group[89,90] in difficult experiments using a reactor. They obtained the following results

$$\sigma(\nu_\mu+e^-)=(1.1\pm0.7)\,E_\nu(\text{GeV})\,10^{-42}\,\text{cm}^2/\text{electron}$$
$$\sigma(\bar\nu_\mu+e^-)=(2.4\pm1.1)\,E_{\bar\nu}(\text{GeV})\cdot10^{-42}\,\text{cm}^2/\text{electron}$$

where σ_{V-A} is the cross section for the usual $V-A$ theory with charged currents:

$$\sigma_{V-A}(\nu_e e^-)=3\cdot\sigma_{V-A}(\bar\nu_e e^-)=1{,}64\cdot10^{-41}E_{\bar\nu}\ (\text{GeV})\text{cm}^2/\text{electron}$$

If we take into account the fact that the reaction (4.9) can also occur via neutral currents besides the usual mechanism via charged currents, the corresponding constants are:

$$G_V=\frac{1}{2}+2\sin^2\theta_W,\quad G_A=\frac{1}{2}. \tag{4.13}$$

In this case the experiment under discussion yields the following bounds for the Weinberg-Salam parameter:

$$0.17<\sin^2\theta_W<0.33. \tag{4.14}$$

In closing this section we should say that, although the experimental data on scattering of neutrinos by electrons have as yet been obtained with low statistics, and most likely should be regarded as qualitative, the very fact of discovery of neutral currents in the weak interaction of leptons is one of the clearest confirmations of the gauge theories which establish a connection between the weak and electromagnetic interactions. Further experiments along this line, both to refine the total cross sections, and to measure the angular and energetic characteristics of the electron, and especially polarization of electrons, are of fundamental interest for establishing the variants of the weak interaction for neutral currents and choosing a model of the interaction.

c. Production of single π-mesons

The reactions of production of single pions in neutrino reactions are next to the elastic processes in the simplicity of their interpretation. They allow one to establish the isotopic properties of the weak current, and they have been calculated in detail within the framework of the $V-A$ theory of production of pion-nucleon systems of small mass in reactions involving charged currents and in the Weinberg-Salam model for reactions involving neutral currents.[91,92]

1) Charged currents. The most recent experimental data on single-pion production reactions in neutrino interactions with hydrogen and deuterium have been obtained by the ANL group.[93] The low energy of the neutrino beam makes it possible to obtain the most clearcut result, since at these energies the cross section for production of two or more pions is relatively small. For neutrinos, the following single-pion reactions with neutrons and protons can occur:

$$\left.\begin{aligned}&\nu_\mu p \to \mu^- p\pi^+,\\ &\nu_\mu d \to \mu^- p\pi^+ (n_s),\end{aligned}\right\} \quad (4.15)$$

$$\nu_\mu d \to \mu^- n\pi^+ (p_s), \quad (4.16)$$

$$\nu_\mu d \to \mu^- p\pi^0 (p_s), \quad (4.17)$$

here (n_s) and (p_s) are the neutron and proton "bystanders."

In the first reaction the pure $I=\frac{3}{2}$ state is realized in the proton-pion system, while a mixture of the $I=\frac{3}{2}$ and $I=\frac{1}{2}$ states is realized in the latter two reactions.

The distribution of the pion-nucleon system with respect to effective masses shows a dominant production of Δ^{++} (1232) in the reaction (4.15) with the cross section $(0.74\pm0.18)\times10^{-38}$ cm^2 for $E_\nu>1$ GeV, whereas formation of a Δ^+ resonance is not observed in the reactions (4.16) and (4.17), with a statistics several times smaller (49 and 55 events, respectively). We also note that Δ^{++} production has been observed also at higher energies ($E_\nu>15$ GeV) in an experiment by the FM group.[72]

The amplitudes in the reactions (4.15)–(4.17) for various charge combinations of the pion-nucleon system can be written in the form

$$\left.\begin{aligned}&A(\pi^+p) = A_3 - (1/\sqrt{5})\,B_3,\\ &A(\pi^+n) = 1/3A_3 + 2/3A_1 + (1/\sqrt{5})\,B_3,\\ &A(\pi^0p) = (\sqrt{2}/3)\,A_3 - (\sqrt{2}/3)\,A_1 + \sqrt{2/5}\,B_3,\end{aligned}\right\} \quad (4.18)$$

where A_1 and A_3 are the isovector amplitudes that lead to the final states $I=\frac{1}{2}$ and $I=\frac{3}{2}$, while B_3 is the hypothetical isotensor exchange amplitude, which assumedly pertains only to $I=\frac{3}{2}$ states.

Analysis of the probabilities of the observed reactions leads to the following conclusions:

a) the triangular inequalities that stem from (4.18) are satisfied under the condition

$$-0.52\pm0.11 \leqslant B_3/A_3 \leqslant 0.23\pm0.07,$$

i.e., the data agree with the absence of isotensor exchange;

b) under the assumption that $B_3=0$, we have for $M_{\pi N}<1.4$ GeV/c^2 the following ratio of the isovector amplitudes and the relative phase:

$$|A_1|/|A_3| = 0.78\pm0.15, \quad \varphi = (92\pm10)^\circ.$$

The numerical values of A_1 and A_3 can be expressed also in the form of the ratios given in Table VII.

We see from the table that one observes a reasonable agreement with the calculations of Adler, whereas one cannot reconcile the data with the absence of final states having the isotopic spin $I=\frac{1}{2}$.

2) Neutral currents. The following reactions can occur in single pion production processes involving neutral currents:

$$\nu p \to \begin{cases}\nu+n+\pi^+,\\ \nu+p+\pi^0,\end{cases} \quad (4.19)$$

$$\nu n \to \nu + n + \pi^0, \quad (4.20)$$

$$\nu n \to \nu + p + \pi^-, \quad (4.21)$$

which must be compared with the corresponding reactions (4.15)–(4.17) for charged currents.

TABLE VII.

R	Experiment	$A_1=0$	Theory
$R^+=\frac{\sigma(\mu^-n\pi^+)}{\sigma(\mu^-p\pi^0)}$	1.01±0.33	0.5	0.77
$R^{+0}=\frac{\sigma(\mu^-n\pi^+ + \mu^-p\pi^0)}{\sigma(\mu^-p\pi^+)}$	0.74±0.15	0.33	0.58

In an experiment with hydrogen and deuterium the ANL group[94] has observed the reactions (4.19) and (4.21) (14 and 17 events, respectively), and they obtained the following relationships:

$$\sigma(\nu p \to \nu n\pi^+ + \nu p\pi^0)/\sigma(\nu p \to \mu^- p\pi^+) = 0.68\pm0.28, \quad (4.22)$$

$$\sigma(\nu n \to \nu p\pi^-)/\sigma(\nu n \to \mu^- n\pi^+) = 0.38\pm0.11. \quad (4.23)$$

The result of the BNL group with the 7-foot bubble chamber for the reaction (4.21) practically coincides with (4.23).[95]

Within two standard deviations, the value of the ratio of (4.22) does not disagree with theory in the WS model, which predicts values for it from 0.15 to 0.44 for the ANL spectrum. The ratio of (4.23) implies that $\sin^2\theta_W>0.15$.[92]

Single pion production in processes involving neutral currents has also been studied in nuclei in an experiment with the Gargamelle chamber and in two electron experiments (CERN, BNL). These data are given in Table VIII, where we have adopted the following notation:

$$R^0 = \sigma(\nu N \to \nu N'\pi^0)/2\sigma(\nu N \to \mu^- N'\pi^0),$$

$$\overline{R}^0 = \sigma(\bar\nu N \to \bar\nu N'\pi^0)/2\sigma(\bar\nu N \to \mu^+ N'\pi^0).$$

In the last column of Table VIII theoretical values have been obtained for $\sin^2\theta_W=0.35$ taking charge-exchange scattering by nuclei into account. In Ref. 97, the authors compare with theory the ratios $r=R^0/\overline{R}^0=0.66\pm0.15$ and the ratio of cross sections $\sigma_N^{\pi^0}(\bar\nu)/\sigma_N^{\pi^0}(\nu)=0.49\pm0.12$, which are least sensitive to nuclear effects. These ratios imply at the 90% confidence level that $0.25<\sin^2\theta_W<0.55$.

In addition to generally testing the WS model, which as can be seen from the presented data, does not contradict experiment, the single-pion processes also give important information on the isotopic structure of the neutral currents.

Some theories[99] assume that the weak neutral current is isoscalar, i.e., transitions with $\Delta I=0$ should dominate in the reactions (4.19)–(4.21). In this case one expects that the ratio $Q^\nu=Q^{\bar\nu}=\pi^0:\pi^-=0.9:1$ for Freon, and the ratio $\sigma(\nu p \to \nu p\pi^0)/\sigma(\nu p \to \nu n\pi^+)=\frac{1}{2}$. An experiment by the GGM group[73] found that $Q^\nu>1.4$; $Q^{\bar\nu}>2.4$. An ANL experiment[94] found $\pi^0:\pi^+$ to be

TABLE VIII.

R^0/experiment	GGM[96]	AP[97]	CIR[98]	Theory[92]
R^0	0.15±0.05	0.40±0.06	0.17±0.04	0.20
$\overline{R}^0$	0.35±0.09	0.61±0.10	0.39±0.18	0.25

3.1 ± 2.1. As we see, the aggregate of these data rules out the isoscalar hypothesis for the neutral currents.

On the other hand, one expects that $Q = 2$ in the case of dominance of the isovector transition amplitude ($\Delta I = 1$). This does not contradict experiment. In this case one should also observe baryon resonances having $\Delta I = \frac{3}{2}$ in the final state. At present the information here is restricted and contradictory owing to the scanty statistics. Thus, in an experiment using the Gargamelle chamber corresponding peaks are found in the invariant-mass distributions in the system $p + \pi^0$ and $p + \pi^-$, both for events involving charged and neutral currents. In an experiment by the BNL group[98] a resonance is visible in the $p\pi^0$ system for charged but not for neutral currents. Apparently, just as for the charged currents, the neutral currents are a mixture of transitions with $\Delta I = 0$ and $\Delta I = 1$.

5. DEEP INELASTIC νN-SCATTERING AND THE QUARK- PARTON MODEL

As we see from the diagram presented below, the kinematics of the process of inelastic scattering involving charged currents is fully defined by the variables $Q^2 = -q^2$, $\nu_H = E_\nu - E_\mu$, E_ν or x, y, $E_\nu (x = Q^2/2m_N\nu_H, y = \nu_H/E_\nu)$:

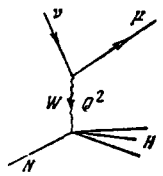

Within the limits of Bjorken scaling ($Q^2 \to \infty$, $\nu_H \to \infty$), the differential distributions over the variables x, y, and E_ν are given by the expression (3.3). Hence, in neutrino interactions, experiment and theory are compared on the basis of the structure functions $F_2(x)$ and $xF_3(x)$ or the differential distributions with respect to x, y, and Q^2. Moreover, since there is a connection between νN and eN scattering, in the deep inelastic region ($Q^2 > 1, W^2 > 4$ GeV^2), the results of eN scattering (structure functions of the nucleon or momentum distributions of the quarks in the nucleon) can be directly compared with νN scattering.

a) Structure functions and momentum distributions of quarks

The structure functions $F_2(x)$ and $F_3(x)$ are related to the cross sections by the equations (3.3). Hence, in order to determine them directly, we must measure the absolute differential distributions jointly for νN and $\bar{\nu} N$ interactions under identical conditions. This has been done up to now only in an experiment at relatively low energies in the Gargamelle bubble chamber at CERN.[100]

First of all we should cite a number of important integral characteristics that follow from the data of this experiment on the total cross sections.

From the data on the total cross sections it was found that

$$\int_0^1 F_2(x)\,dx = \int_0^1 [q(x) + \bar{q}(x)]\,dx = 0.52 \pm 0.03. \tag{5.1}$$

This result means that the active constituents of the nucleon (quarks or antiquarks) carry away only about half the momentum of the nucleon, and the remaining part of the momentum is carried away by the gluons. The proton consists of (u, u, d) quarks and the neutron of (d, d, u) quarks. The integral baryon and electric charges of protons imply the following sum rules:

$$\begin{aligned} &\int_0^1 [u(x) - \bar{u}(x)]\,dx = 2, \\ &\int_0^1 [d(x) - \bar{d}(x)]\,dx = 1. \end{aligned} \tag{5.2}$$

The results (5.1) and (5.2) imply that

$$\begin{aligned} &\int xu(x)\,dx \approx 0.3, \\ &\int xd(x)\,dx \approx 0.15. \end{aligned} \tag{5.3}$$

The value of the parameter $B = 0.90 \pm 0.05$[61,62] and the relationships (5.1) and (3.8) imply that

$$\int_0^1 \bar{q}(x) = 0.02 \pm 0.01. \tag{5.3'}$$

The quark-parton model, as well as the more general properties of the interactions (the hypothesis of conserved vector current, and the equality of the vector and axial-vector coupling constants) establish the following relationships between νN and eN scattering:[23]

$$\begin{aligned} F_2^{\nu p}(x) + F_2^{\nu n}(x) &= R_2[F_{2,1}^{ep}(x) + F_{2,1}^{en}(x)], \\ xF_3^{\nu p}(x) + xF_3^{\nu n}(x) &= R_3[F_2^{ep}(x) - F_2^{en}(x)]. \end{aligned} \tag{5.4}$$

The coefficient R_2 in the simple quark model equals $18/5 = 3.6$ (more exactly, taking into account the current involving a change of strangeness $\Delta S = 1$ and the quark-antiquark "sea", we have $R_2 = 3.45$). An experiment on eN scattering[101] yields:

$$\int_0^1 F_2^{eN}\,dx = \frac{1}{2}\int_0^1 [F_2^{ep}(x) + F_2^{en}(x)]\,dx = 0.15 \pm 0.01. \tag{5.5}$$

Hence, experimentally, upon comparing (5.1) and (5.5) we have $R_2 = 3.6 \pm 0.3$. This agrees with the value expected from the quark model and corresponds to a fractional charge of the quarks.

A determination of the structure functions proper, i.e., their dependence on x, has been carried out by the GGM group by analyzing 2656 νN and 1063 $\bar{\nu} N$ interactions for $E_{\nu,\bar{\nu}} > 1$ GeV. However, only 200 and 29 events respectively belonged to the region of eN scaling ($Q^2 > 1, W^2 > 4$ GeV^2). Although the functions $F_2(x)$ and $xF_3(x)$ found with these cutoffs agree well with the analogous data on eN scattering, more abundant statistics are needed for more detailed comparison. Hence in subsequent analysis all events were used, but the variable x was replaced everywhere by the variable x':

$$x' = \frac{q^2}{2m_N\nu_H + m_N^2}. \tag{5.6}$$

As the theory implies,[102] this new variable corresponds better to the low energy region also in eN scattering. Actually the approach to scaling is attained more

rapidly with respect to the variable x' than to x.

Moreover, it was assumed that $F_i^{\nu N} = F_i^{\bar{\nu} N} = F_i$, which corresponds to charge symmetry.

Figure 20 shows not the structure functions themselves, but the quark-antiquark momentum distributions in the nucleon as found directly from νN scattering in terms of the relation given by the parton model:

$$\bar{q}(x') = x'\bar{n}(x') = \frac{1}{2}[F_2(x') - x'F_3(x')],$$
$$q(x') = x'n(x') = \frac{1}{2}[F_2(x') + x'F_3(x')], \qquad (5.7)$$

where $n(x)$ is the probability that a quark possesses the fraction x of the total longitudinal momentum of the nucleon. The curves in Fig. 20 represent a theoretical recalculation[103-106] from the analogous distributions found in eN scattering. The areas under these curves represent the fraction of the momentum of the nucleon carried away by all the quarks or antiquarks. As can be seen from Fig. 20, the shape and absolute values of the structure functions and momentum distributions of the quarks in νN scattering correspond well with eN scattering as studied in the deep inelastic region.

The distribution $xF_3(x)$ allows us to test the Gross-Llewellyn-Smith sum rule:[107]

$$\frac{1}{2}\int [F_3^{\nu p}(x) + F_3^{\nu n}(x)]\,dx = \frac{3}{2}(1+\cos^2\theta_C), \qquad (5.8)$$

which corresponds to the number of valence quarks in the nucleon $(N-\bar{N}) = 3$ and is a test of the hypothesis of fractional charge of quarks. For the integral (5.8) in the given experiment the value 3.2 ± 0.6 was found for $E_\nu > 1$ GeV. This agrees well with the quark model.

The data of the experiment permitted them to test also Adler's sum rule.[108] It was found that

$$\frac{d\sigma^{\nu N} - d\sigma^{\nu N}}{dq^2} < \frac{0.3G^2}{\pi},$$

which does not contradict the expected value 0.008 ($SU(3)$ scheme) or 0.087 ($SU(4)$ scheme).

In closing this section we shall present some preliminary data on the energy-dependence of the integral characteristics $\int F_2 dx$ and $\int xF_3 dx$, which were recently obtained in the BEBC bubble chamber at CERN.[153] As we have stated above, in this experiment the total cross-sections $\sigma_C^{\nu N}$ and $\sigma_C^{\bar{\nu} N}$ were measured at several energies and the values of the integrals were calculated using the following expressions:

$$\int F_2\,dx = 0.94\,(\sigma_{C\lambda}^{\nu N} + \sigma_C^{\bar{\nu}\bar{N}})\,\frac{1}{2\sigma_0},$$
$$\int xF_3\,dx = 0.94\,(\sigma_C^{\nu N} - \sigma_C^{\bar{\nu}\bar{N}})\,\frac{1}{\sigma_0}. \qquad (5.9)$$

Figure 21 presents the data of this experiment together with the data of the GGM group. As can be seen from the diagram, the integral of F_2 is approximately constant over a broad energy range, and no sharp change in the function (threshold behavior) is observed at any energy, as might happen in the case of production of new heavy particles (b-quarks). The energy-dependence of the integral of F_3 indicates a small but noticeable decline. As the authors point out, both relationships agree with the predictions of the asymptotically-free field theories, which explain the breakdown of scaling of deep inelastic lepton-nucleon scattering. We shall treat this problem in greater detail in the next section.

b) The y-distribution

Even without absolute normalization to the total cross sections, the study of the differential distributions over the scaling variables is of great interest for elucidating the model of the nucleon and the limiting behavior of the structure functions. These distributions have been measured in several experiments, including the Gargamelle[101] bubble chamber and the 15-foot (Batavia) bubble chamber, and also in experiments with electronic detectors of the HPWF, CITF, and CERN-Dortmund-Heidelberg-Saclay (CDHS) groups. Table IX and Figs. 22–23 give the fundamental conditions and results of the experiments. As the general expression (3.3) implies, at high energies (after integration with respect to x) the y-distribution is given by the expression

$$\frac{d\sigma^{\nu N(\bar{\nu}N)}}{dy} = \sigma_0\Big[\int_0^1 F_2(x)\,dx\Big]\Big[1 - (1 \mp B)\Big(y - \frac{1}{2}y^2\Big)\Big]. \qquad (5.10)$$

When $B = 1$, the distribution does not depend on y in the case of νN interaction and is proportional to $(1-y)^2$ for $\bar{\nu}N$ interactions. Usually the experimental results are compared with (5.10) and the parameter B is obtained. Table IX gives the values of this parameter.

Figure 22 gives the data of the GGM group only for events in the scaling region, and Fig. 23 for all events, including elastic ones. The solid curves are calculated by (5.10) with $B = 0.9$, with the known form factors for

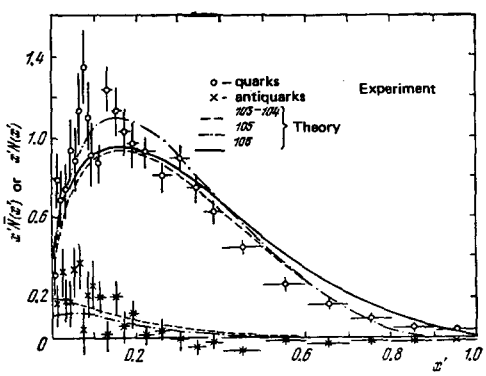

FIG. 20. Distribution functions of quarks and antiquarks as functions of x as obtained from the experiment of GGM group, together with the predictions of theory.

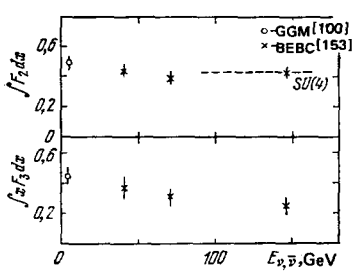

FIG. 21. Energy dependence of the integrals of the structure functions.

TABLE IX.

Experiment, group	Beam	Target	Energy range of ν or $\bar{\nu}$; mean energy, GeV		Number of events		Values of the parameter B	
			Mean E	High E values E	Mean E	High E	Mean E	High E
HPWF[110]	ν $\bar{\nu}$ (1/3 horn+ +2/3 triplet)	C, H, Fe	$10<E_\nu<30$ $10<E_{\bar{\nu}}<30$	>70, $\langle E\rangle_\nu=126$ >70, $\langle E\rangle_{\bar{\nu}}=106$	946 991	1905 310	0.6 ± 0.3 0.94 ± 0.09	0.83 ± 0.20 0.41 ± 0.13
CITF[111,154]	ν $\bar{\nu}$ $\bar{\nu}$ (dichromatic)	Fe		$E_\nu=50-150$ $\langle E\rangle_{\bar{\nu}}^{\nu}=52$ $\langle E\rangle_{\bar{\nu}}=150$		2000 1000 200		$B_\nu\approx1$ 0.80 ± 0.06 0.65 ± 0.10
15′-bubble chamber, FM[112]	ν (horn)	H_2	$15<E_\nu<200$ $\langle E\rangle_\nu\approx40$		450		flat y distribution $B_\nu\approx1$	
15′-bubble chamber, AMP[113]	$\bar{\nu}$ (horn)	H_2	$5<E_{\bar{\nu}}<30$	30	332		0.91 ± 0.08	0.82 ± 0.14
15′-bubble chamber, FIMS[114]	$\bar{\nu}$ (horn)	$H_2+21\%$ Ne	$10<E_{\bar{\nu}}<50$	50	613		0.78 ± 0.06	$0.62^{+0.14}_{-0.20}$
CDHS[156]	ν $\bar{\nu}$ (dichromatic)	Fe		40 – 200		36 400 11 900		$B_\nu\approx1$ $B_{\bar{\nu}}\approx0.8$

elastic scattering taken into account. As can be seen from these diagrams, with the distribution of (5.10), good agreement is observed in both cases. As can be seen from Table IX and Fig. 24, agreement with (5.10) is also observed at high energies for νN interactions, i.e., none of the data contradict a flat or almost flat distribution. (We must note that the sensitivity of the data to changes in the parameter B is in this case considerably lower than for the $\bar{\nu}N$ interactions.)

The situation differs for antineutrino-nucleon interactions at high energies. In 1975 the HPWF group[67,109] found a number of anomalies in deep inelastic $\bar{\nu}N$ scattering, and, in particular, a considerable change in the shape of the y-distribution with increasing energy. Figure 25 shows the most recent data of this group.[110] As can be seen from Fig. 25a, for the energy range $E_{\bar{\nu}}<30$ GeV, the data correspond to the parameter $B^{\bar{\nu}}=0.94$, which agrees with the data of the Gargamelle group. However, with increasing antineutrino energy the y-distribution flattens out, as we see from Fig. 25b, and the mean value $\langle y\rangle$ correspondingly increases with increasing energy (Fig. 25c).

In view of the fundamental importance of this fact, which could be explained by production of new hadrons differing from charmed particles (b-quarks),[19]

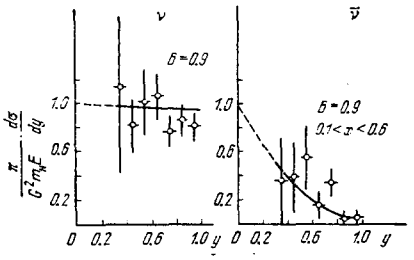

FIG. 22. The y-distributions (data of the GGM group) for νN and $\bar{\nu}N$ interactions for events having $Q^2>1$ GeV^2, $W^2>4$ GeV^2.

$\bar{\nu}N$ scattering has recently been studied intensively in other experiments.

Figure 26a presents the data obtained by the FIMS group using a bubble chamber from which we see that the shape of the y distribution varies less sharply than was observed in the HPWF experiment. Figure 27 shows the energy-dependence of the parameter $B^{\bar{\nu}}$, including the data of all experiments with the exception of the data of the HPWF experiment, including new results obtained at CERN,[153,156] as well as by the CITF group at Batavia.[154] As can be seen from Fig. 27, the results of the experiments using bubble chambers (we note that the y-distribution was not measured in the experiment with the BEBC chamber, and the value of the parameter B was obtained by comparing the integrals $B=\int F_2dx/\int xF_3dx$) and of an experiment using the CITF

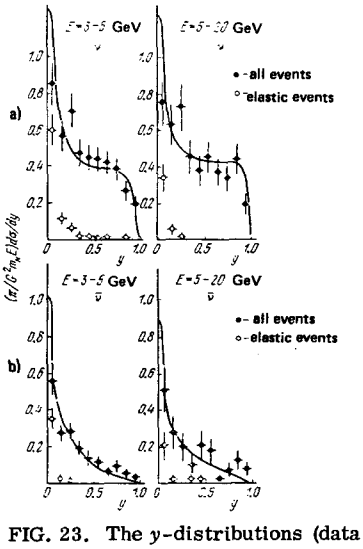

FIG. 23. The y-distributions (data of the GGM group) for all events in νN (a) and $\bar{\nu}N$ (b) interactions and for different energy ranges.

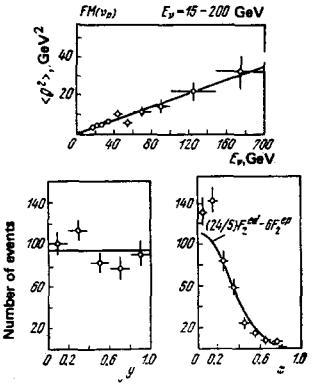

FIG. 24. Distributions with respect to the variables Q^2, x, and y (data of the FM group) for νp interactions.

electronic detector exhibit a smooth variation of the parameter B with increasing energy, but appreciably smaller in magnitude than was observed by the HPWF group. The data of the electron experiment of the CERN group show no change at all in the parameter B over the broad energy range 40–200 GeV.

Thus we can take it at present that, although there are some contradictions in the recent experimental data, the large y-anomaly observed in the experiment of the HPWF group does not exist.

Another type of a y-anomaly observed by the HPWF group[62,65] consists of the fact that $d\sigma/dy^{\nu N} \neq d\sigma/dy^{\bar{\nu} N}$ in the region of x values close to zero. This has also recently been tested in experiments at CERN[156] and Batavia.[154] Neither group found any appreciable violations of charge symmetry. Thus, the data of Ref. 154 show that the quantities

$$\sigma_{y=0} = \frac{1}{E}\frac{d\sigma}{dy}\Big|_{y=0}$$

for νN and $\bar{\nu} N$ interactions agree with an accuracy of about 5% in the energy range 50–200 GeV. The results are approximated by the relationship

$$\sigma_{y=0} = (0.744 \pm 0.040) - (0.00035 \pm 0.00040)\, E_{\nu,\bar{\nu}} \cdot 10^{-38}\ \text{cm}^2/\text{GeV}.$$

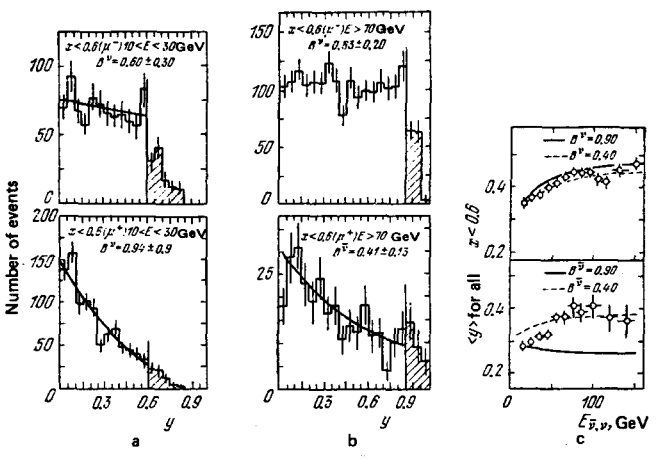

FIG. 25. The y-distributions (data of the HPWF group) for νN and $\bar{\nu} N$ interactions in the energy range below 30 GeV (a) and above 50 GeV (b) and the energy-dependence of the mean value of the variable y ($\langle y \rangle$) (c). Solid curves—calculation for the conditions of the given experiment by Eq. (5.10).

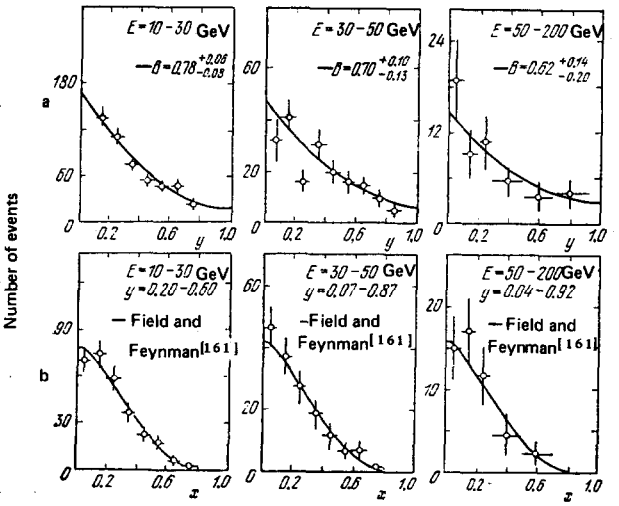

FIG. 26. The y, x-distributions in $\bar{\nu} N$ interactions (data of the FIMS group) for different energy ranges. Solid curves in Fig. b—theoretical relationships from Ref. 161.

c) The x, ν-distributions. Violation of scaling

In the limit of Bjorken scaling, Eq. (3.3) implies that the x-distribution is determined by the relationship

$$\frac{d\sigma^{\nu N,\ \bar{\nu} N}}{dx} = \frac{1}{3}\sigma_0 [2F_2(x) \pm xF_3(x)]. \qquad (5.11)$$

The distribution over the variable v, which is defined as

$$v = xy = \frac{E_\mu (1 - \cos\theta_\mu)}{m_N} = \frac{q^2}{E_\nu}\frac{1}{2m_N}, \qquad (5.12)$$

and the mean value $\langle v \rangle$ in the scaling region should not depend on the energy. In view of the fact that there are no direct experimental data for neutrino-nucleon scattering at high energies on the structure functions $F_i(x, q^2)$, the differential x, v-distributions (absolute or relative) give useful information on the extent to which scaling is obeyed in the studied region of energies and of q^2.

Experimental data on the stated distributions are given in Figs. 24, 26, and 28–33, together with theoretical predictions and with data on electroproduction.

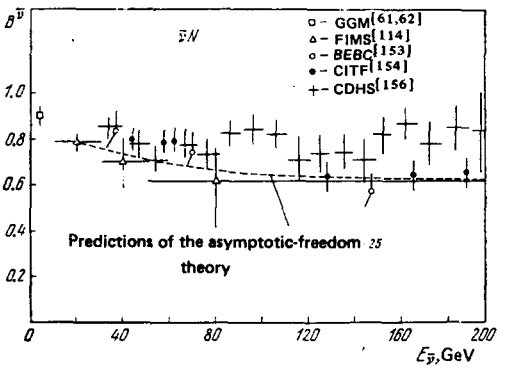

FIG. 27. Experimental values of the parameter B obtained in different experiments as a function of the energy (dotted curve—asymptotic-freedom theory[25]).

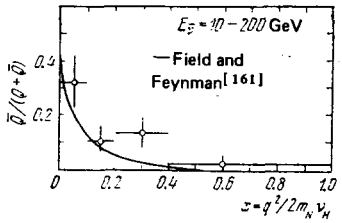

FIG. 28. Relative contribution of the antiquarks to $\bar{\nu}N$ scattering as a function of x, as obtained in an experiment of the FIMS group.[114] Solid curve—theoretical estimate.[161]

Before we proceed to interpret the neutrino data, let us consider the effects of deviation from exact Bjorken scaling in electroproduction. The first clear proof that the structure functions $F_i(x, q^2)$ in the range $q^2 \sim 1-20$ GeV^2 show deviations from pure scaling ($F_i(x, q^2) = F_i(x)$) was obtained in an experiment on μN scattering performed at Batavia at the two energies of 56 and 150 GeV.[163] Similar effects have also been observed in the scattering of electrons[164] and muons by hydrogen and deuterium.[165,166] In these experiments the characteristic feature of the violation of scaling is the fact that the functions $F(x, q^2)$ increase for small x ($x < 0.2$) and decrease for large x ($x > 0.2$) with increasing q^2. We note that the results for the structure functions $F_1(x, q^2)$ are less accurate than for $F_2(x, q^2)$, but their trends of variation are the same. The deviation from scaling in muon-nucleon scattering is described by the following formula:

$$\frac{\partial \ln F_2(x, q^2)}{\partial \ln (q^2/q_0^2)\, \partial \ln (x/x_0)} = -a, \tag{5.13}$$

where $a \approx 0.07-0.10$, $q_0^2 = 3$ GeV^2, and $x_0 \approx 0.17$. Several possibilities exist for comparing neutrino-nucleon scattering at high energies with electroproduction.

One of them, which was recently realized by Field and Feynman,[161] consists of finding the distribution functions of the quarks $u(x)$, $d(x)$, and $s(x)$ by an appropriate parametrization of the electroproduction data in analogy with the procedure discussed above in analyzing the structure functions obtained in the experiment of the Gargamelle group. Then the $d\sigma/dx$ distribution for $\nu N(\bar{\nu}N)$ scattering is reconstructed from them. In view of the scant experimental data on electroproduction at $x > 0.8$ and the weaker sensitivity of the structure functions in eN scattering to the quarks

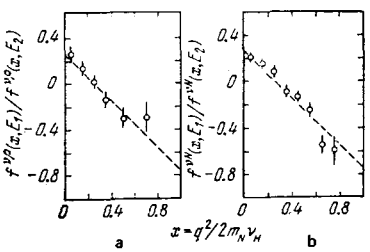

FIG. 29. The dependence on x of the ratio of the function $f(x)$ as determined from Eq. (5.16) at two energies. a) The ratio for $\langle E \rangle \sim 40$ GeV (FM[112]) and $\langle E \rangle \sim 2$ GeV (ANL[167]) for νp interactions; b) the ratio for $\langle E \rangle \sim 60$ GeV (HPWF[110]) and $\langle E \rangle \sim 4$ GeV (GGM[100]) for νN interactions. Dotted curves—0.25–x, relationships, which correspond to breakdown of scaling in electroproduction.

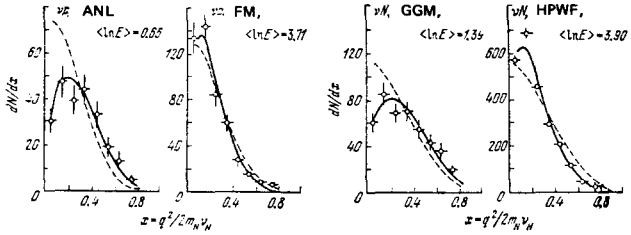

FIG. 30. The x-distribution for the same experiments as in Fig. 29. Solid curves—the expected relationships from electroproduction (Eq. (5.17)); the dotted curves were found for the case without breakdown of scaling.

of the "sea" ($u\bar{u}, d\bar{d}, s\bar{s}$) in the region $x < 0.2$, several assumptions were made in this study concerning the behavior of the distribution functions of the quarks and antiquarks in the stated regions.

Figure 26b shows the experimental data for dN/dx obtained by the FIMS group,[114] in which the solid curves are calculated by formulas from the paper by Field and Feynman.

Figure 28 shows an analogous comparison of the data for the x-dependence of the relative contribution of the antiquarks to the scattering. As we see from these diagrams, experiment and the theoretical predictions agree well.

Perkins *et al.*[159] have recently made a somewhat different comparison of the deviation from scaling in neutrino and electron-muon scattering over a broad energy range. The authors of this study found that the data on eN and μN scattering in the region $q^2 \sim 1-40$ GeV^2 and $x = 0-0.8$ can be approximated by the formula

$$F_2^{eN,\,\mu N}(x, q^2) = F_2(x, q_0^2)\left(\frac{q^2}{q_0^2}\right)^{f(x)}, \tag{5.14}$$

where we have

$$f(x) = \frac{\partial \ln F_2^{eN,\,\mu N}(x, q^2)}{\partial \ln q^2} \approx 0.25 - x \tag{5.15}$$

and $q_0^2 = 3$ GeV^2. They showed that if the structure functions in νN scattering have the same form, then

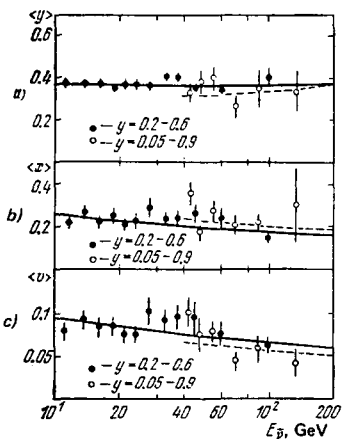

FIG. 31. Mean values of the scaling variables y, x, and v as functions of the energy (FIMS experiment[114]). The curves in Fig. a were obtained from the equation $B = (0.86 \pm 0.05) - (0.0038 \pm 0.0012)\, E$. The solid curves in Figs. b and c are $E^{-0.15}$ relationships.

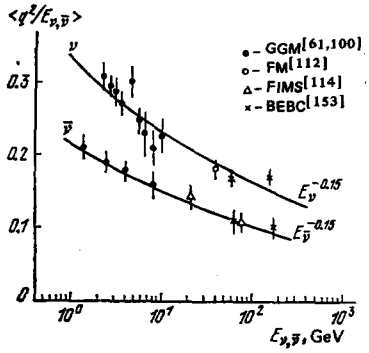

FIG. 32. Energy-dependence of the quantity $\langle q^2/E\rangle$ for νN and $\bar\nu N$ interactions.

$$\frac{\partial \ln[(1/\sigma)\, d\sigma/dx]}{\partial \ln E} = f(x). \tag{5.16}$$

Figure 29a gives the ratio of the quantities $f(x)$ for the experiments on νp scattering at FM[112] and ANL,[167] which were performed at substantially different neutrino energies, respectively $\langle E\rangle_\nu \sim 40$ GeV and $\langle E\rangle_\nu \sim 2$ GeV. Figure 29b gives an analogous comparison for νN scattering in experiments by HPWF[65] ($\langle E\rangle_\nu \sim 60$ GeV) and GGM[100] ($\langle E\rangle_\nu \sim 4$ GeV). The broken line in these diagrams represents the relationship (5.15) as found in electroproduction. As can be seen from these diagrams,

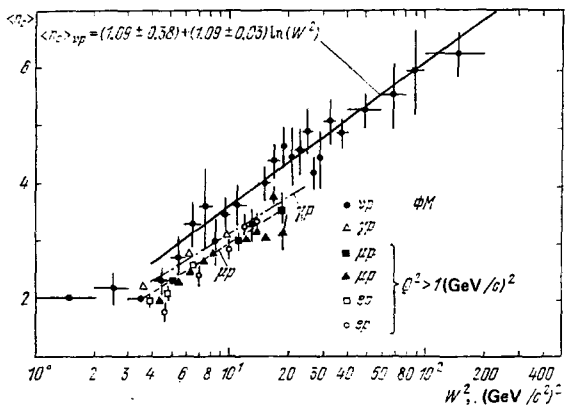

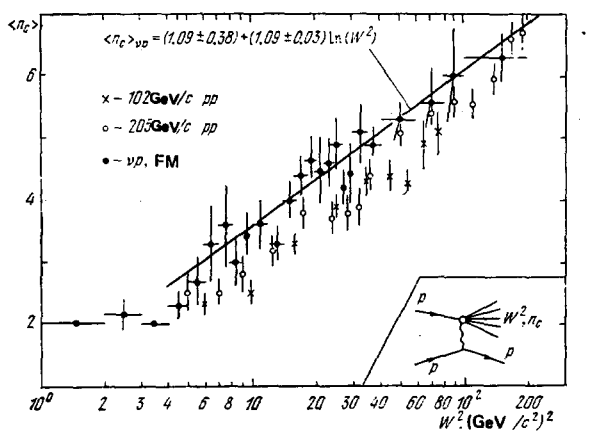

FIG. 33. Dependence of the mean multiplicity $\langle n_c\rangle$ of hadrons on the square of the invariant mass W^2 of the hadrons for νp interactions as found in an FM experiment for neutrino energies 15–200 GeV. The experimental data for $\langle n_c\rangle$ are also given for other types of interactions.

the violation of scaling in νN scattering is of the same nature as in eN and μN scattering. The authors of Ref. 159 also showed that the shape of the x-distribution in the given method of parametrization is obtained in the form

$$\frac{dN^{\nu p,\ \nu N}}{dx}(x,\ E) = \frac{F_2^{\nu p,\ \nu N}(x,\ q_0^2)}{1+f(x)} \left(\frac{2m_N E x}{q_0^2}\right)^{f(x)}, \tag{5.17}$$

Here the $F_2(x, q_0^2)$ relationship is given by the expressions

$$F_2^{\nu p}(x,\ q_0^2) = \frac{24}{5} F_2^{ed}(x,\ q_0^2) - 6F_2^{ep}(x,\ q_0^2),$$
$$F_2^{\nu N}(x,\ q_0^2) = \frac{9}{5} F_2^{ed}(x,\ q_0^2). \tag{5.18}$$

Figure 30 shows the dN/dx distributions for the experiments discussed above in which the solid curves correspond to (5.17). We can see that the experimental and expected distributions agree well. The broken curve in this diagram shows a calculation that assumed that $F_2^{\nu p, \nu N}(x) = F_2^{\nu p, \nu N}(x, q_0 = 3)$, i.e., a case without scaling violation.

As can be seen from all the experimental data discussed above the shape of the x-distribution varies very little especially in the restricted energy range covered by any given single experiment (e.g., the experiment of the FIMS group and Field and Feynman's analysis; Fig. 26). The difference becomes more appreciable if one analyzes the set of all experiments in a broader energy region and goes over to the mean values $\langle x\rangle$ and $\langle v\rangle$, which are measured more accurately. We should expect on the basis of violations of scaling in electroproduction that the mean values $\langle x\rangle$ and $\langle v\rangle$ (or $\langle q^2/E\rangle$) should diminish with increasing energy. It has been shown[114] that if one employs the parametrization of Perkins *et al.*,[159] then these quantities should vary with energy according to the power law E^{-b}, where $b \approx 0.15$. This actually holds both for νN and for $\bar\nu N$ interactions, as can be seen from Figs. 31 and 32, which present data obtained with bubble chambers.

Thus the fundamental conclusion that we can draw at present consists of the idea that neutrino-nucleon interactions manifest qualitatively the same deviations from exact scaling in the region $q^2 = 0.5$–30 GeV^2 as do the eN and μN scattering.

The explanation of violation of scaling in lepton-nucleon interactions is actually the object of hadron field theory within the framework of the quark-gluon model (quantum chromodynamics, asymptotic-freedom theory). Without discussing the details of this problem, we wish to note the following.

Deviation from scaling in neutrino-nucleon scattering in the high energy region might be associated with production of new particles (heavy quarks). Such effects would be considerably stronger in νN interactions than in electromagnetic interactions. Hence we can conclude that the effects of heavy quarks are not manifested within the limits of the considerable experimental errors.

One of the obvious corrections to the simple quark-

parton model is the one involving taking into account the masses of the quarks and of the nucleons. As recent calculations[168] show, such corrections can explain only a part of the effect of violation of scaling, although they present serious theoretical grounds for the replacement of variables $x \to x'$ at low energies, as has been discussed in subsection *a* of this section.

In the current theory,[25,169] the main source of deviation from exact scaling is the q^2-dependence of the quark-gluon constant $\alpha(q^2)$. In the asymptotic-freedom theory $\alpha(q^2)$ approaches zero as $(\ln q^2/\mu^2)^{-1}$ for large q^2. The unknown parameter μ^2 arises from the renormalization of the theory. The moments of the structure functions vary as $\ln(q^2/\mu^2)^{-\gamma_i}$, where γ_i is a positive constant of the order of unity. Perhaps, as has been discussed in Ref. 159, a fair description of all the data by the relationship (5.14) implies that the parameter μ^2 is small ($\mu^2 \ll 1$ GeV^2).

At present the developing theory of quark-gluon interactions already provides a number of interesting predictions for neutrino-nucleon scattering.[170] However, they can be tested only in future, more accurate neutrino experiments using hydrogen and deuterium targets.

d) Structure of the hadron block

In addition to studies of distributions involving the scaling variables of the muon, the study of hadrons being produced is of great interest in inclusive processes. Experimental information on the properties of the hadron shower is currently very limited, and has been obtained mainly in experiments with bubble chambers.

The experiment of the Fermi-Michigan (FM) group[118] already discussed above, has measured the multiplicity of charged hadrons in a νp experiment. Figure 33 shows the dependence of the mean multiplicity of charged particles $\langle n_c \rangle$ on the square of the invariant mass of the hadrons W^2. It also presents the data for ep, μp, and γp scattering. The data on νp scattering are well approximated by a logarithmic dependence, and they reflect the overall rule that the mean number of hadrons coming from excitation of nucleons does not depend on the nature of the interaction, but only on the invariant mass of the hadron system.

It was found in Ref. 118 that the mean multiplicity does not depend on Q^2 for fixed values of W^2. The mean number of π^0 mesons per event in this experiment increases as a function of the multiplicity of charged particles from 1.5 ± 0.3 for three-prong events to 3.2 ± 0.8 for nine-prong events. This also agrees with the data of hadron-hadron experiments.

Figure 34a shows the distributions of the invariant cross sections with respect to the Feynman scaling variable $x_F = P_L^*/P_{L,\max}^*$ in the center-of-mass system of the hadrons for νp interactions.[72] Here we also present (Fig. 34b) the data of the hadron experiments. Figure 34 exhibits good agreement of all the data. This can be interpreted in such a way that the virtual regeons (pp collisions) and the intermediate W-boson (νp reactions) manifest themselves in the same way in multiple production processes.

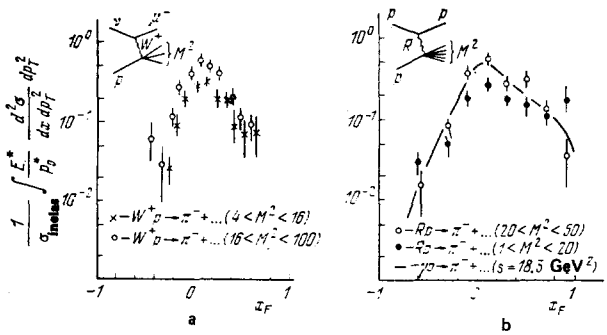

FIG. 34. Dependence of the invariant cross sections on the Feynman variable x_F for νp interactions (data of the FM group) (a) and for pp interactions (b).

We note that the mean transverse momentum of the π-mesons with respect to the direction of the total hadron momentum is 0.30 GeV/c, and the distribution of events with respect to $p_\perp^2$ is described by an exponential with an index of ~5.5.

One can obtain more interesting predictions on the behavior of the characteristics of individual π-mesons and nucleons in neutrino-nucleon collisions using the quark-parton model.[23,161]

The experimentally observable functions of the hadrons are determined by the momentum distribution of the quarks in the hadron prior to collision, and by functions $D(Z)$ that characterize the conversion of the quark into real hadrons after collision (according to Feynman's definition, $D(Z)$ is the decay function of the quark). Here $Z = E_a/\nu_H$ is the fraction of the total energy ν_H of the hadrons carried away by an individual hadron. Here the differential cross section for production, e.g., of π-mesons in νp collisions has the form

$$\begin{aligned} \frac{d^2\sigma_\nu^{\pi^+}}{dx\,dz} &= cx\left[d(x)\,D_u^{\pi^+}(Z) + \tfrac{1}{3}\,\bar{u}(x)\,D_{\bar{d}}^{\pi^+}(Z)\right], \\ \frac{d^2\sigma_\nu^{\pi^-}}{dx\,dz} &= cx\left[d(x)\,D_u^{\pi^-}(Z) + \tfrac{1}{3}\,\bar{u}(x)\,D_{\bar{d}}^{\pi^-}(Z)\right]. \end{aligned} \tag{5.19}$$

Charge symmetry implies that

$$D_u^{\pi^+} = D_{\bar{d}}^{\pi^+}, \quad D_u^{\pi^-} = D_{\bar{d}}^{\pi^-}. \tag{5.20}$$

Therefore the ratio of the yields of π^+ to π^- mesons

$$R_\pi\left(\frac{\pi^+}{\pi^-}\right) = \frac{D_u^{\pi^+}(Z)}{D_u^{\pi^-}(Z)} \tag{5.21}$$

does not depend on x.

Figure 35a shows the data obtained in an experiment using the Gargamelle chamber,[119] while Fig. 35b shows those from an experiment by the FM group[72] (15-foot chamber, H_2). As can be seen, Eq. (5.21) is satisfied within the limits of the considerable experimental errors.

Equation (5.19) implies that, if we neglect the contribution of the antiquarks, the functions $D(Z)$ are determined simply by the experimental differential distributions $d\sigma_\nu^\pi/dz = N^\pi(x, Z) = D^\pi(Z)$. The functions $N(Z)$ are given in Fig. 36, both for νp interactions[72] and for

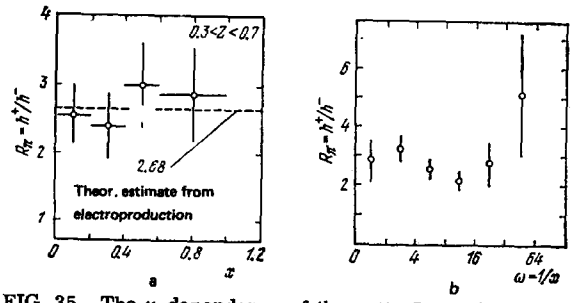

FIG. 35. The x-dependence of the ratio $R_\pi(h^+/h^-)$ in an experiment of the GGM group (a) and in an experiment of the FM group (b).

ep interactions,[171] which agree within the experimental limits of error with one another and with the theoretical estimates.[161]

6. NEUTRINO INTERACTIONS AND NEW PARTICLES

This section will present only the fundamental experimental results in the search for new particles in neutrino interactions, since a special review will be devoted to this topic.

a) Fundamental mechanisms of production of charmed particles

Within the framework of the $SU(4)$ scheme[12] following the introduction of the c quark, the fraction of the current responsible for production of charmed particles has the form

$$(J_\mu)_{\Delta c=1} = \bar{c}\gamma_\mu(1-\gamma_5)(-d\sin\theta_C + s\cos\theta_C). \tag{6.1}$$

The elementary transitions between the quarks that are allowed by the current of (6.1) and by the conservation laws lead to the following expressions for the differential cross sections for production of C-particles in an isoscalar target:

$$\begin{aligned}\frac{d^2\sigma^{\nu N}(C)}{dx\,dy} &\sim x[\sin^2\theta_C\cdot(u+d)+2\cos^2\theta_C\cdot s+2\bar{c}(1-y)^2],\\ \frac{d^2\sigma^{\bar{\nu}N}(C)}{dx\,dy} &\sim x[2c(1-y)^2+\sin^2\theta_C\cdot(\bar{u}+\bar{d})+2\cos^2\theta_C\cdot\bar{s}].\end{aligned} \tag{6.2}$$

We can estimate in a crude approximation from (6.2) the overall yield of C-particles by adopting the values of (5.3) for the mean moments of the quarks.[25] This yield proves to be about 10% for νN interactions and 20% for $\bar{\nu}N$ interactions. However, the estimates of the cross sections for production by the quarks of the "sea" are very uncertain,[16] and we should treat them as upper limits.

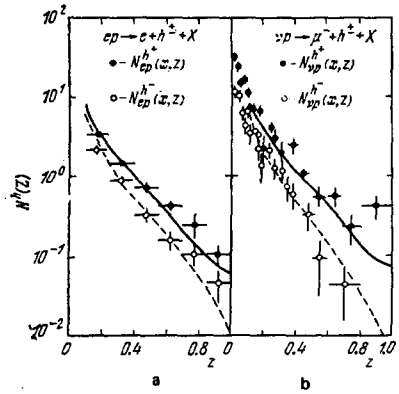

FIG. 36. Differential distributions $d\sigma/dz = N^h(z,x)$ as a function of z for ep interactions (a) and for νp interactions (b). Curves—theoretical estimates.[161]

A series of studies[120,121] has also treated the cross section for production of charmed F^* mesons ($F^* = c\bar{s}; 1^-$) in concrete reactions, and in particular, as resulting from the mechanism of diffraction production, i.e.,

$$\nu + N \to \mu^- + F^{*+} + N. \tag{6.3}$$

The absolute yield of F^* in reaction (6.3) should decline with increasing q^2, while the relative yield increases with q^2.[16] An estimate of the cross section for the reaction (6.3)[120] at energies above the threshold (~10 GeV) leads to the relatively small cross sections of $2\times10^{-3}\sigma_{tot}$.

Exclusive production of baryons in the reactions

$$\nu p \to \mu^- + C_1^{++}, \quad \nu n \to C_1^+(C_0^+) + \mu^-, \quad \nu p \to \mu^- + K^+ + C_{0,1}^{++} \tag{6.4}$$

is expected at the level of relative cross-sections $\lesssim 10^{-3}$.[120]

An important feature of the C-particles is their relatively large probability of decay by lepton modes, which is estimated to amount to about 10%.

Figure 37 presents the schemes of production and decay of the charmed particles.[22]

b) Production of strange particles in inclusive and exclusive channels

The mechanisms of production and decay of charmed particles should result in the final hadron state being enriched by strange particles.

At present the available experimental data on production of strange particles have been obtained only in experiments using bubble chambers. Owing to the small cross sections for production of strange particles, all together only tens of events have been observed in these experiments and they mainly pertain to events of the $V^0(K^0,\Lambda)$ type.

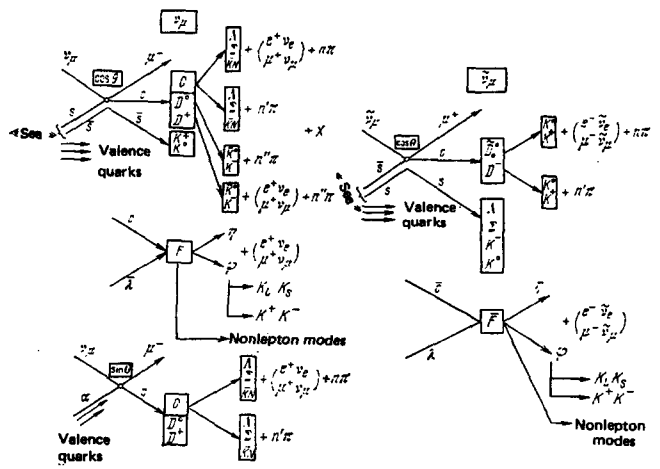

FIG. 37. Diagrams of production and decay of charmed particles in $\nu N(\bar{\nu}N)$ interactions.

TABLE X.

Bubble chamber	Target	Beam	$\langle E_{\nu,\bar{\nu}}\rangle$, GeV	Number of detected events, V^0	$Y_{V^0}=\frac{N_{V^0}}{N_{CC}}$ (%)	References
"Gargamelle"	CF_3Br	ν	2.5	53	5.1±1.5	122, 123
12′, ANL	H_2D_2	ν	1	7	4±1.5	124
7′, BNL	H_2D_2	ν	2.5	10	3±1	125
15′, FNAL	H_2	ν	38	38	16±3	126
15′, FNAL	H_2	$\bar{\nu}$	23	8	13±5	113
15′, FNAL	H_2+21% Ne	$\bar{\nu}$	30	48	16±3	127

Table X presents the data of experiments on the yield of V^0 events corrected for the undetectable modes of decay of K^0 and Λ particles, and also for the efficiency of detection of the visible modes of decay. (For experiments at low energy, one takes only the number of CC events for which $W>2$ GeV).

Figure 38a shows the relative yield of V^0 events with correction for the efficiency of detection (but without taking into account the invisible decay modes) as a function of the invariant mass W of the hadrons, both for neutrino reactions, and for γN, μN, and $\pi^- p$ interactions. Figure 38b shows the distribution with respect to invariant mass of events involving strange particles (histogram) and of all events involving charged particles (continuous curve), as obtained in an antineutrino experiment with the 15-foot bubble chamber of the FIMS group.

We can draw from the data of Table X and Fig. 38 the general conclusion that the yield of strange particles at high energies increases more rapidly with energy for νN and $\bar{\nu}N$ interactions than for the other interactions, and that for $W>4$ GeV it exceeds by (30–40)% the data of the hadron experiments. It is as yet an open question whether this is associated with production of charmed particles. In experiments of the GGM, FM, and FIMS groups searches were made for charmed particles in the spectra of the invariant masses of different combinations of strange particles with hadrons ($\Lambda\pi$, $\Lambda\pi\pi$, $\Lambda\pi\pi\pi$, γ, $K\pi$, $K\pi\pi$, etc.). These distributions showed no peaks of masses above 1.5 GeV, and upper limits were found for production and decay involving the given modes at the 1% level.

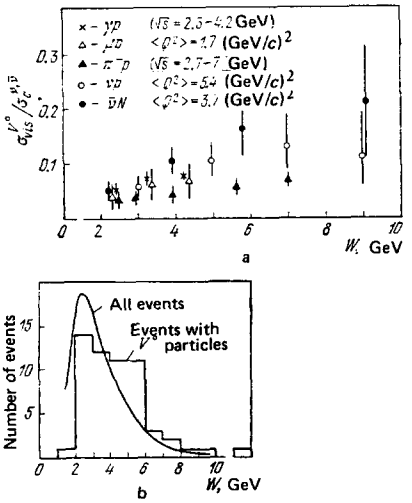

FIG. 38. Dependence on the invariant mass W of the hadrons of the relative cross section for production of V^0 particles in $\bar{\nu}N$ interactions for events having detectable V^0 particles (FIMS group). The curve in Fig. b is the distribution with respect to the invariant mass of the hadrons for all events in $\bar{\nu}N$ interactions.

The only event in exclusive reactions that indicates production of a new particle decaying into hadrons is the case found in an experiment with the 7-foot cryogenic bubble chamber of BNL[128] at $E_\nu=13.5$ GeV:

$$\nu p \to \mu^- C^{++} \to \mu^- + \Lambda\pi^+\pi^+\pi^+\pi^-. \qquad (6.5)$$

In this event $\Delta S=-\Delta Q$. It can be interpreted as production of the charmed baryon $\sum_c^{++}$[77] or of a F-meson.[129]

Events analogous to reaction (6.5) have also been sought in other experiments. In a neutrino experiment in the 15-foot FNAL bubble chamber filled with hydrogen[126] not a single event of the type (6.5) was found with a substantially larger flux of ν of energy above 10 GeV. The authors give an upper bound for single production at the 90% confidence level:

$$\frac{N(\Delta S=-\Delta Q)}{N_{CC}}<3.6\%$$

In an experiment with the Gargamelle chamber all together 106 single Λ-hyperons were observed. These events appear mainly because of the low efficiency of simultaneous detection of two strange particles. The authors estimated that the expected number of associative production events is (64 ± 18). Hence we can ascribe the excess (42 ± 20) to production of a charmed baryon, and here the yield is estimated to be (2 ± 1)%.

One of the possible candidates for a charmed baryon was found also in a study[172] by the ANL group.

c) Observation of lepton pairs in neutrino interactions

The most definite proof of production of new particles in neutrino experiments is the observation of two-lepton events.

$$\nu_\mu(\bar{\nu}_\mu)+N\to\mu^-(\mu^+)+\mu^+(\mu^-)+X. \qquad (6.6)$$

Two (6.6) events were first observed by the HPWF group in 1974.[131] The search for $(\mu\mu, \mu e)$ lepton pairs has subsequently been conducted not only by this group, but also in other neutrino experiments.

Tables XI and XII present a summary of all the experiments, their conditions and observed processes, while Fig. 39 gives the energy-dependence of the yield of two-lepton events.

At present the best experiment for studying two-muon

TABLE XI. $\mu\mu$-Events.

Group	Beam	$E_\nu, \bar{\nu}$, GeV	Type of events	Number of $\mu\mu$ events	Background, %	Number of 1μ events	Energy cutoff of muons, GeV**	Yield $Y = [N(2\mu)/N(1\mu)] \cdot 10^2$
HPWF[131-133]	ν $\bar{\nu}$ ν $\bar{\nu}$	40—200	$\mu^-\mu^+$ $\mu^-\mu^-$ $\mu^+\mu^-$ $\mu^+\mu^+$	64 7 10 3	~ 25	~ 10^4	$E_{\mu_1,\mu_2} > 4$	0.8 ± 0.3 0.08 ± 0.04 2 ± 1
CITF[134,135]	ν ν ν $\bar{\nu}$	30—220	$\mu^-\mu^+$ $\mu^-\mu^-$ $\mu^-\mu^+\mu^-$ $\mu^+\mu^-$	90 (13) *) (2) (2) 33 (8)	~ 20	$1.2\cdot10^4$ $0.6\cdot10^4$	$E_{\mu_1} > 12$ $E_{\mu_2} > 2.4$	~ 1 ~ 0.1 ~ 1
IS[136,161]	ν	10—30	2μ	40	~ 100	$0.5\cdot10^4$	$E_{\mu_1\mu_2} > 1$,	0.64 ± 0.20 $W > 2$
CDHS[173]	ν $\bar{\nu}$ ν $\bar{\nu}$	40—200	$\mu^-\mu^+$ $\mu^+\mu^-$ $\mu^-\mu^-$ $\mu^+\mu^+$	257 58 47 9	~ 10 ~ 60	$5.3\cdot10^4$ $1.5\cdot10^4$	$E_{\mu_1,\mu_2} > 4.5$	~ 1 ~ 1 $\sim \leqslant 0.1$

Note: The numbers indicated for the experiment of the CITF group in parentheses correspond to events in which 2 (or 3) muons enter the magnetic part of the spectrometer and their charge is definitely identified.
Note: A muon of the "correct sign" (e.g., μ^- in νN interactions) is taken for μ_1, and one of the "wrong sign" (μ^+ in νN interactions) for μ_2.

events is one by the CDHS group[173] that was performed with the 1000-ton SPS detector at CERN. Figure 39b presents separately the data on the yields obtained in this experiment, together with the detection efficiency function obtained taking into account the production of charmed D mesons.[142]

The experimental study of the properties of two-lepton processes leads to the following conclusions.

1. The kinematic features observed for two-lepton events, such as the shift of the x-distribution toward smaller values of x, the flat y-distribution, the difference of the energies and transverse momenta of the two muons ($\langle E\rangle_{\mu_1} \gg \langle E\rangle_{\mu_2}, \langle p_\perp\rangle_{\mu_1} > \langle p_\perp\rangle_{\mu_2}$), the strong anticorrelation in the azimuthal angle of separation of the two muons, and the change in the invariant mass of the muons with increasing energy, indicate that the process (6.6) proceeds via production at the hadron vertex and the subsequent lepton or semilepton decay of charmed hadrons of mass ~2 GeV/c^2.

2. The μe events that have been observed in bubble chambers have the same properties; it was found in addition that such events are accompanied in a considerable number of cases by strange particles, so that the mean multiplicity of K mesons is $\langle K\rangle = 1.5$–2, as is expected in the production and decay of charmed mesons.

3. The observed yield of two-muon events, which is about 1–1.5% for $E_{\nu,\bar{\nu}} > 40$ GeV, is the same for νN and $\bar{\nu}N$ interactions. This corresponds to the fact that the cross section for production of charmed particles in neutrino interactions amounts to about 10% of the total cross section involving charged currents, and the probability of their decay by lepton channels amounts to

TABLE XII. μe-Events.

Group	Beam	$\langle E_\nu, \bar{\nu}\rangle$, GeV	Type of events	$N(\mu e)$	Background (number of events)	$N(1\mu)$	Energy cutoff of electrons, GeV	Yield of events $Y = \frac{N(\mu e)}{N(1\mu)} \cdot 10^2$
GGM[123,137]	ν_μ	2.5	$\mu^-e^+V^0$ μ^-e^+ μ^-e^- $\nu_\mu e^+$	3 17 26 4	0.09 ± 0.03 6.1 ± 1.8 26.0 ± 4.0 3.7 ± 1.0	$4.8\cdot10^3$ for $W > 2$ GeV	0.2	(0.3 ± 0.13) (for $W > 2$ GeV)
BNL[138]	ν_μ	2.5	μ^-e^+	7	2 ± 1	$1.5\cdot10^4$	1.5	~ 0.3 (for $W > 2$)
BCHW[139]	ν_μ	30	$\mu^-e^+V^0$ μ^-e^+ $\nu_\mu e^+V^0$	9 4 2 } 15	1	$4\cdot10^3$	0.4	$f^{-1}\times0.63\times$ $\times(1\pm0.33)$ $(f \sim 0.5)$ $E_\nu > 5$ GeV $E_e > 0.8$ GeV
CB[140, 139]	ν_μ	30	$\mu^-e^+V^0$ μ^-e^+	9 61	6	$2\cdot10^4$	> 0.4	0.5 ± 0.15
FIMS[141]	$\bar{\nu}_\mu$	30	$\mu^+e^-V^0$ μ^+e^- μ^+e^+ $\bar{\nu}_\mu e^-$	0 1 (?) 1 (?) 6	0.02 0.2 ± 0.2 0,03 4	$1.1\cdot10^3$	> 0.2	< 0.3 < 0.5 < 0.5

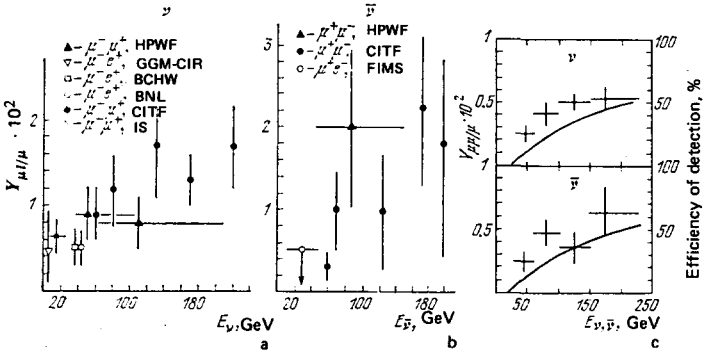

FIG. 39. Relative yield of $\mu\mu$ and μe events as a function of $E_{\nu,\bar{\nu}}$. a) All experiments given in Tables XI and XII except the experiment of the CDHS group; b) experiment of the CDHS group.

(20–30)%.

4. Other mechanisms that can yield lepton pairs (Fig. 40), such as the production and decay of vector mesons (a), direct production of lepton pairs[143] (b), production of a W-boson (c), and production of a heavy lepton[144] (d) are ruled out at the level of accuracy of the given experiments.

5. The question of the observation of lepton pairs of like charge ($\mu^-\mu^-$ in νN, or $\mu^+\mu^+$ in $\bar{\nu}N$ interactions)[132] remains open, since such events in the experiments of the CDHS group at CERN[173] can basically be explained by background processes.

6. The three-lepton events observed up to now by the CITF[135] and HPWF[157] groups pose the question of the possible production of a heavy lepton with subsequent cascade decay.

On the whole, the data of all the experiments investigating two-lepton events agree with the 4-quark GIM scheme for the semilepton weak interactions.[12,22] (Fig. 40e).

It would seem that further neutrino experiments will be able to establish more concretely precisely which charmed mesons and baryons are produced and what are their decay schemes.

d) Other experiments

A number of other experiments closely adjoin the problem of new phenomena in neutrino physics discussed in this section, and we shall review them briefly below.

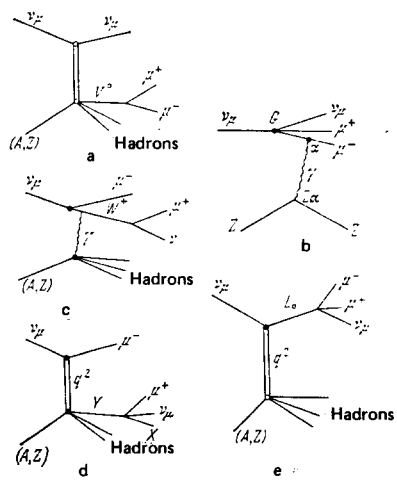

FIG. 40. Possible diagrams for production of two leptons in νN interactions.

In an experiment to study neutrinos of cosmic origin performed in South India using a counter method deep underground,[145] five events were observed that had a vertex in the air near the apparatus. The authors assumed that these events arise from the decay of a new particle produced in neutrino interactions that has a mass of ~2 GeV/c^2 and a lifetime $\tau \sim 10^{-9}$ sec. Ref. 146 gives another possible interpretation, namely production in the atmosphere of a heavy, long-lived lepton $L^0(m_{L^0} \sim 2$–3 GeV/c^2, and $\tau > 10^{-5}$ sec).

The hypothesis concerning production of neutral long-lived leptons has been tested in neutrino experiments using accelerators.[147,148] An experiment at CERN using the Gargamelle chamber was set up under conditions of "absorption" of the proton beam in the shielding,[149] resulting in neutrinos of ordinary origin from the decay of π- and K-mesons being suppressed. The HPWF group performed an experiment with the usual neutrino arrangements, but with the aim of seeking decays of L^0 leptons, the liquid scintillator was removed from one section of the detector and this space was filled with helium. These two experiments, in which the reduced intensity of neutrinos or protons was considerably higher (by 2–3 orders of magnitude) than in the cosmic ray experiment, gave a negative result. Recently one event was observed among 1000 $\nu_\mu N$ events in a neutrino experiment with the SKAT chamber.[150] In particular, this could be interpreted as the production and decay of a short-lived ($\tau \sim 6 \times 10^{-12}$ sec) heavy neutral lepton with a mass of $M \sim 2$ GeV/c^2:

$$\nu_\mu + N \to L^0 + p + 2\pi^0,$$
$$\qquad\quad \hookrightarrow \mu^- + e^+ + \nu_e.$$

This interpretation is based on the fact that the $\mu^- e^+$ pair is separated from the interaction vertex by 0.5 cm.

In closing this section, we also point out the great promise of neutrino experiments using photoemulsions. Actually, if the new particles have lifetimes of 10^{-14}–10^{-12} sec and decay paths of 10–1000 μm, then they can be directly observed only in photoemulsions. Experiments of this type which employ large stacks of photoemulsion (50–150 kg), together with external electronic detectors, are performed at the Serpukhov, FNAL, and CERN accelerators.

One possible short-lived charged object has already been discovered in an emulsion experiment at FNAL

(decay path 182 μm, $\tau \sim 6 \times 10^{-13}$ sec, possible decay schemes $D(1.87) \to K^0K^+K^-\pi^\pm$, $\sum_c(2.48 \to \Lambda^0K^+K^-\pi^\pm)$. The discovery of several other short-lived events of this type would be a final proof of the production of charmed particles.

Finally, one of the interesting problems of neutrino physics is that of the degree of conservation of lepton charge (the distinction between ν_μ and ν_e, and that between ν and $\bar{\nu}$). As analysis shows, the fundamental information on this subject is derived from the experimental level to which the rule forbidding the decay $\mu \to e\gamma$ is obeyed. Pontecorvo[152] has proposed a more sensitive test of the degree of conservation of lepton charge that consists of seeking neutrino oscillations, i.e., transitions in vacuo of one type of neutrino into another. One of the realistic formulations of such experiments involves experiments with solar neutrinos, although the possibility is not ruled out of conducting such experiments using accelerators.

7. CONCLUSION

The review that we have given evinces considerable progress in the physics of neutrino studies during the past several years.

The discovery of neutral currents in semilepton and pure lepton processes and their qualitative study is one of the most important advances in the physics of weak interactions at high energies.

The observation of two-lepton events accompanied by an elevated yield of strange particles is a rather cogent proof of the existence of particles having the new quantum number of charm. The study of deep inelastic neutrino-nucleon scattering agrees generally with the quark-parton-gluon model at high energies.

All these problems are currently the topic of further intensive studies in various energy ranges with a new generation of electronic neutrino detectors and with expansion of the scope of studies using large bubble chambers. Neutrino experiments have been furthered by the recent placing in operation of a new 400-GeV accelerator at CERN.

The vigorous development of experimental and theoretical studies of neutrino processes allows us to hope that this interesting field of elementary particle physics will very soon substantially deepen our understanding of the weak interactions and the structure of hadrons.

[3)] Abbreviations used: Frascati—International Conference on Instrumentation for High Energy Physics, Frascati, Italy, 1973; London—Proc. of the 17th International Conference on High Energy Physics, London, 1974; Paris—La Physique du Neutrino a haute Energie, Ecole Polytechnique, Paris, 1975; Stanford—Proc. of the International Symposium on Lepton and Photon Interactions at High Energies, Stanford, 1975; Aachen—Proc. of the International Conference "Neutrino—76", Aachen, 1976; Tbilisi—Proc. of the 18th International Conference on High Energy Physics, Tbilisi, 1976; "Neutrino-77"—International Conference, USSR, North Caucasus, June 1977.

[1]G. Danby *et al.*, Phys. Rev. Lett. **9**, 36 (1962); **10**, 260 (1963).
[2]J. K. Bienlein *et al.*, Phys. Lett. **13**, 80 (1964).
[3]D. C. Cundy *et al.*, *ibid.*, **B31**, 478 (1970).
[4]R. P. Feynmann, M. Gell-Mann, Phys. Rev. **109**, 193 (1958); R. Marshak, E. Sudershan, *ibid.*, p. 1860; L. B. Okun', Slaboe vzaimodeĭstvie élementarnykh chastits (Weak Interactions of Elementary Particles), Fizmatgiz, M., 1963 (Engl. Transl., Israel Program for Scientific Translations, Jerusalem, 1965); T. D. Lee and C. S. Wu, Slabye vzaimodeĭstviya (Weak Interactions), "Mir", M., 1968.
[5]M. Gell-Mann, Phys. Rev. **125**, 1067 (1962); N. Cabibbo, Phys. Lett. **10**, 513 (1963).
[6]S. Weinberg, Phys. Rev. Lett. **19**, 1264 (1967); A. Salam, in Elementary Particle Theory, Proc. of 8th Nobel Symposium, Stockholm, 1968, p. 367.
[7]C. N. Yang, R. Mills, Phys. Rev. **96**, 191 (1954); S. Weinberg, Rev. Mod. Phys. **46**, 255 (1974).
[8]P. Higgs, Phys. Rev. Lett. **13**, 508 (1964).
[9]B. A. Arbuzov, Tbilisi, v. II, B194.
[10]J. Ellis *et al.*, Preprint CERN, 1976.
[11]A. Salam, Supplement to the Russ. Transl. of: K. Nishijima, Fundamental Particles, Benjamin, New York, 1964 ("Mir", M., 1965, p. 429).
[12]S. L. Glashow, J. Iliopoulos, and L. Maiani, Phys. Rev. **D2**, 1285 (1970).
[13]M. K. Gaillard, B. W. Lee, J. L. Rosner, Rev. Mod. Phys. **47**, 277 (1975); G. A. Altarelli, N. Cabibbo, L. Maiani, and R. Petronzio *et al.*, Phys. Lett. **B48**, 435 (1974).
[14]J. E. Augustin *et al.*, Phys. Rev. Lett. **33**, 1406 (1976).
[15]J. J. Aubert *et al.*, *ibid.*, p. 1404.
[16]V. I. Zakharov, B. L. Ioffe, and L. B. Okun', Usp. Fiz. Nauk **117**, 227 (1975) [Sov. Phys. Usp. **18**, 757 (1975)].
[17]G. Goldhaber *et al.*, Phys. Rev. Lett. **37**, 255 (1976); I. Peruzzi *et al.*, *ibid.*, p. 569.
[18]M. L. Perl, Phys. Rev. Lett. **35**, 1489 (1975); Phys. Lett. **B63**, 466 (1976).
[19]H. Harari, *ibid.* **B57**, 265 (1975); R. M. Barnett, Phys. Rev. **D14**, 70 (1976); V. Barger *et al.*, *ibid.*, p. 1276; Z. Babaev and V. Zamiralov, Yad. Fiz. **26**, 391 (1977) [Sov. J. Nucl. Fiz. **26**, 391 (1977)]; I. Barinov and G. Volkov, Preprint of the Institute of High-Energy Physics 76-98, Serpukhov, 1976.
[20]A. Slavnov, Tbilisi, v. II, T12.
[21]J. Pati, A. Salam, Phys. Rev. D **8**, 1240 (1973); A. Salam, Tbilisi, v. II, N. 91.
[22]S. Gershtein, *ibid.*, v. II, B125.
[23]R. P. Feynman, Photon-Hadron Interactions, Benjamin, Reading, Mass., 1972 (Russ. Transl., "Mir", M., 1975). J. D. Bjorken, Phys. Rev. **179**, 1547 (1969); V. I. Zakharov, Tbilisi, v. II, B69.
[24]N. N. Bogolyubov, B. V. Struminskiĭ, and A. N. Tavkhelidze, Preprint of the JINR (OIYaI)R-2141, Dubna, 1965; L. B. Okun', Adrony i kvarki (Hadrons and Quarks), MIFI, M., 1974.
[25]L. Maiani, in: École d'ete de physique des part., GIF-SUR-YVETTE, 1975, p. 60. G. Altarelli, Tbilisi, v. II, B66.
[26]L. G. Hyman, Paris, p. 183.
[27]P. Musset, CERN Rept. TC-L/Int. 74-9 (1974).
[28]N. P. Somois, Stanford, p. 527.
[29]E. V. Eremenko *et al.*, Paris, p. 331; D. G. Baratov et al., Zh. Tekh. Fiz. **47**, 991 (1977) [Sov. Phys. Tech. Phys. **22**, 591 (1977)].
[30]F. A. Nezrick, NAL Rept. **8**, 1974, p. 1.
[31]D. G. Baratov *et al.*, Preprint of the Institute of High-Energy Physics 76-87, Serpukhov, 1976.
[32]A. Benvenuti *et al.*, Paris, p. 397.
[33]B. C. Barish, CALT 68-535 (6th Hawaii Topical Conference in Particle Physics, August 1975).
[34]Experiments at CERN in 1976, Geneva, 1 Sept. 1976.
[35]N. I. Bozhko *et al.*, Preprint of the Institute of High-Energy Physics 76-89, Serpukov, 1976.
[36]D. Bloess *et al.*, Nucl. Instr. and Meth. **91**, 605 (1971).

[37]A. P. Bugorskiĭ *et al.*, Preprint of the Institute of High-Energy Physics 72-72, Serpukhov, 1972.
[38]R. Imlay *et al.*, in: Proc. of the 17th Intern. Conference on High Energy Physics, London, 1974; A Benvenuti *et al.*, Phys. Rev. Lett. **37**, 189 (1976).
[39]T. D. Lee, C. N. Yang, *ibid.*, **4**, 307 (1960); Y. Yamaguchi, Proc. Theor. Phys. **23**, 1117 (1960); N. Cabbibo, R. Gatto, Nuovo Cimento **15**, 304 (1960); T. D. Lee, C. N. Yang, Phys. Rev. **126**, 2239 (1962); J. J. Sakurai, UCLA/73/TEP/79, 1973.
[40]H. Faissner, E. Frenzel, T. Hansl *et al.*, Aachen, p. 223.
[41]H. Faissner, Balaton, v. 1, p. 116; M. Baldo-Ceolin, *ibid.*, p. 166.
[42]a) L. Sulak, in: Proc. of Calorimeter Workshop, FNAL, Batavia, 1975, p. 155; b) H. H. Williams, in: Proc. of Intern. Conference on Production of Particles, Madison, University of Wisconsin, 1976, p. 45.
[43]W. Lee, Aachen, p. 319.
[44]A. E. Asratyan *et al.*, Preprint of the Institute of High-Energy Physics 75-105, Serpukhov, 1975.
[45]A. Benvenuti *et al.*, Nucl. Instr. and Meth. **125**, 447, 457 (1975).
[46]B. C. Barish, Preprint CALT 68-535, 1975.
[47]J. Engler *et al.*, Nucl. Instr. and Meth. **106**, 189 (1973).
[48]H. Faissner, in Proc. Dubna 1964, v. II, p. 352; B. C. Barish *et al.*, see Ref. 42b, p. 229.
[49]F. R. Huson, Paris, p. 357.
[50]E. P. Kuznetsov, Preprint of the JINR (OIYaI)10-4269, Dubna, 1968.
[51]U. P. Reinhard, Frascati, p. 3.
[52]P. Prugne, *ibid.*, p. 13. R. Greogoire, *ibid.*, p. 85.
[53]A. Tomasaitis, K. Teager, *ibid.*, p. 92.
[54]W. Fowler, in: Proc. of Intern. Conference on BC Technology, ANL, 1970, p. 774.
[55]H. Burmeister, D. Cundy, CERN TC-L. Int. Rep. 72-1 (1975); G. Myatt, CERN/ECFA/72-4, v. II, 1972, p. 117; F. Nezrick *et al.*, Phys. Rev. **14D**, 5 (1976).
[56]R. J. Cence *et al.*, Preprint LBL-4816, UH-511-217 (1976).
[57]P. F. Ermolov, in Trudy Mezhdunarodnoĭ shkoly fizikov (Proceedings of the International School of Physicists), Baku, 1976, p. 22.
[58]F. J. Hasert *et al.*, Phys. Lett. **B46**, 138 (1973); Nucl. Phys. **B73**, 51 (1974).
[59]J. D. Bjorken, E. A. Paschos, Phys. Rev. **185**, 1975 (1969); **D1**, 3151 (1970).
[60]C. G. Callan, D. G. Gross, Phys. Rev. Lett. **22**, 156 (1969).
[61]T. Eichten *et al.*, Phys. Lett. **B46**, 274, 281 (1973).
[62]D. Perkins, Stanford, p. 571.
[63]S. J. Barish *et al.*, *ibid.*, p. 511.
[64]B. C. Barish *et al.*, Phys. Rev. Lett. **35**, 1316 (1975); Preprint CALT 68-535 (1975).
[65]A. Benvenuti *et al.*, Phys. Rev. Lett. **32**, 125 (1974); D. Cline, in: Proc. of Intern. Conference on High Energy Physics, Palermo, p. 335.
[66]A. Benvenuti *et al.*, Phys. Rev. Lett. **37**, 189 (1976).
[67]A. Benvenuti *et al.*, *ibid.*, p. 1095.
[68]S. J. Barish *et al.*, Preprint ANL-HEP-CP-75-38 (1975).
[69]E. J. Cazzoli, Paris, p. 317.
[70]M. Haguenauer, *ibid.*, p. 327.
[71]G. Myatt, D. N. Perkins, Phys. Lett. **B34**, 542 (1971).
[72]B. Roe, Rept. on APS DPF Coll, BNL (1976); Tbilisi, v. II, B112.
[73]R. Musset, *ibid.* B87. J. Blietschau *et al.*, Nucl. Phys. **B118**, 218 (1977).
[74]B. C. Barish *et al.*, Phys. Rev. Lett. **34**, 538 (1975); Tbilisi, v. II, B109.
[75]A. Benvenuti *et al.*, Phys. Rev. Lett. **32**, 800 (1974); **37**, 1039 (1976).
[76]L. M. Sehgal, Nucl. Phys. **B65**, 141 (1973); C. N. Albright, *ibid.*, **B70**, 486 (1974).
[77]A. De Rujula, Tbilisi, v. II, N 111.
[78]G. Feinberg, in: Lectures on Astrophysics and Weak Interactions, v. 12, Waltham, Brandeis University, 1963, p. 277.
[79]S. J. Barish *et al.*, Rep. ANL-HEP-CP-75-40 (1975).
[80]M. Rollier, Paris, p. 349.
[81]A. Del Guerra *et al.*, Daresbury Preprint DL P256 (1976).
[82]S. Weinberg, Phys. Rev. **D5**, 1412 (1972).
[83]V. M. Shekhter, Usp. Fiz. Nauk **119**, 593 (1976) [Sov. Phys. Usp. **19**, 645 (1976)].
[84]W. Lee *et al.*, Phys. Rev. Lett. **37**, 186 (1976).
[85]D. Cline *et al.*, *ibid.*, p. 252.
[86]D. Cline *et al.*, *ibid.*, p. 648.
[87]F. J. Hasert *et al.*, Phys. Lett. **B46**, 121 (1973); Nucl. Phys. **114**, 189 (1976).
[88]L. M. Seghal, *ibid.*, B70, 61 (1974); Phys. Lett. **B48**, 60 (1974).
[89]H. Faissner, Tbilisi, v. II, B114, Aachen, p. 223.
[90]F. Reines, H. S. Gurr, H. W. Sobel, Phys. Rev. Lett. **37**, 315 (1976).
[91]S. L. Adler, Ann. Phys. (N.Y.) **50**, 189 (1968); P. A. Schreiner, F. Hoppel, Phys. Rev. Lett. **30**, 339 (1973); Nucl. Phys. **B58**, 333 (1973).
[92]H. A. Albright *et al.*, Phys. Rev. **D7**, 2220 (1973); S. L. Adler, *ibid.* **D9**, 229 (1974). S. L. Adler *et al.*, *ibid.*, p. 2125.
[93]J. Campbell *et al.*, Phys. Rev. Lett. **30**, 335 (1973); A. F. Garfinkel *et al.*, Paris, p. 311. S. J. Barish *et al.*, Phys. Rev. Lett. **36**, 179 (1976).
[94]S. J. Barish *et al.*, *ibid.* **33**, 448 (1974); L. Hyman, Phys. Paris, p. 183. S. J. Barish, Aachen, p. 374.
[95]E. G. Cazzoli, Paris, p. 239.
[96]F. J. Hasert *et al.*, Phys. Lett. **B59**, 485 (1975); P. Musset, CERN/EP/Phys. 76-10 (1976).
[97]Aachen-Padova Collab. Tbilisi, 1180/B3-50; H. Faissner *et al.*, Phys. Lett. **B68**, 377 (1977).
[98]W. Lee *et al.*, Phys. Rev. Lett. **38**, 202 (1977).
[99]J. Sakurai, Phys. Rev. **D9**, 250 (1974).
[100]H. Deden *et al.*, Nucl. Phys. **B85**, 269 (1975).
[101]A. Bodek *et al.*, Phys. Rev. Lett. **30**, 1087 (1973); G. Miller *et al.*, Phys. Rev. **D5**, 528 (1972).
[102]D. Bloom and F. Gilman, Phys. Rev. Lett. **25**, 1140 (1970).
[103]R. McElhaney, S. F. Tuan, Phys. Rev. **D8**, 2267 (1973).
[104]J. T. Dakin, G. J. Feldman, *ibid.*, p. 2862.
[105]G. Altarelli *et al.*, Nucl. Phys. **B69**, 531 (1974).
[106]P. Landshoff, J. Polkinghorne, Phys. Lett. **B34**, 66 (1971).
[107]D. J. Gross, C. H. Llewellyn-Smith, Nucl. Phys. **B14**, 337 (1969).
[108]S. L. Adler, Phys. Rev. **143**, 1144 (1966).
[109]A. Benvenuti *et al.*, Phys. Rev. Lett. **33**, 984 (1974); **34**, 575 (1975).
[110]A. Benvenuti *et al.*, *ibid.* **36**, 1478 (1976).
[111]B. Barish *et al.*, Tbilisi, v. II, **B44**.
[112]J. P. Berge *et al.*, Phys. Rev. Lett. **36**, 639 (1976).
[113]M. Derrick *et al.*, *ibid.*, p. 936; AMP-Collab, Tbilisi, 618/B3-25.
[114]J. P. Berge *et al.*, Phys. Rev. Lett. **39**, 382 (1977).
[115]R. Kögerler, D. Schildknecht, CERN TH. 2247 (1976).
[116]R. E. Taylor, Stanford, p. 679. W. B. Atwood, SLAC Report 185 (1975).
[117]V. Sciulli, CALT 68-520 (1975).
[118]J. W. Chapman *et al.*, Phys. Rev. Lett. **36**, 124 (1976).
[119]D. Candy, London, p. IV 131.
[120]B. W. Lee, Preprint FERMILAB-Conf.-75/78-THY (1975).
[121]B. A. Arbuzov *et al.*, Yad. Fiz. **21**, 1322 (1975) [Sov. J. Nucl. Phys. **21**, 682 (1975)].
[122]H. Deden *et al.*, Phys. Lett. **58B**, 361 (1975).
[123]H. Deden *et al.*, Preprint CERN/EP/PHYS 77-2 (1977).
[124]S. J. Barish *et al.*, Phys. Rev. Lett. **33**, 1446 (1974).
[125]R. B. Palmer *et al.*, Aachen, p. 405.
[126]J. P. Berge *et al.*, Phys. Rev. Lett. **36**, 127 (1976); C. T. Coffin, *et al.*, Tbilisi, 315/B3-31.
[127]FIMS-Collab, Tbilisi, 1158/B3-48.
[128]E. G. Cazzoli *et al.*, Phys. Rev. Lett. **34**, 1125 (1975).

[129]B. W. Lee, Preprint FNAL 75/38-THY (1975).
[130]B. Knapp *et al.*, Phys. Rev. Lett. **37**, 882 (1976).
[131]B. Aubert *et al.*, London, p. 201.
[132]A. Benvennuti *et al.*, Phys. Rev. Lett. **34**, 419, 597; **35**, 1199, 1203 (1975).
[133]D. Cline, Invited Talk given at APS Meeting at BNL, October 1976.
[134]B. C. Barish *et al.*, Phys. Rev. Lett. **36**, 939 (1976).
[135]B. C. Barish *et al.*, Preprint CALT 68-567 (1976); Phys. Rev. Lett. **38**, 577; **39**, 981 (1977).
[136]A. S. Vovenko, Tbilisi, v. II, B92.
[137]S. Blietschau *et al.*, Phys. Lett. **B60**, 207 (1976); H. Deden *et al.*, *ibid.* **B67**, 474 (1977).
[138]W. Lee *et al.*, Aachen, p. 319.
[139]J. von Krogh *et al.*, Phys. Rev. Lett. **36**, 710 (1976); M. L. Stivenson, Tbilisi, v. II, **B88**. P. Bosetti *et al.*, *ibid.* **38**, 1248 (1977).
[140]C. Baltay *et al.*, *ibid.* **39**, 62.
[141]J. P. Berge *et al.*, Phys. Rev. Lett. **38**, 266 (1977).
[142]L. Sehgal, P. Zerwas, *ibid.* **36**, 399 (1976).
[143]G. von Gehlen, Nuovo Cimento **30**, 859 (1963).
[144]A. Pais, S. B. Treiman, Phys. Rev. **D9**, 1459 (1974).
[145]M. R. Krishnaswamy *et al.*, Phys. Lett. **B57**, 105 (1975).
[146]A. de Rujula, S. Georgi, S. Glashow, Phys. Rev. Lett. **35**, 628 (1975).
[147]H. Faissner *et al.*, Phys. Lett. **B60**, 401 (1976).
[148]A. Benvenuti *et al.*, Phys. Rev. Lett. **35**, 1486 (1975).
[149]B. M. Pontekorvo, Zh. Eksp. Teor. Fiz. **69**, 452 (1975) [Sov. Phys. JETP **42**, 229 (1975)].
[150]D. S. Baranov *et al.*, Yad. Fiz. **26**, 110 (1977) [Sov. J. Nucl. Phys. **26**, xxx (1977)]; Phys. Lett. **B70**, 269 (1977).
[151]E. H. Burhop *et al.*, Preprint ULB-VNB, 11HE-76 (1976).
[152]B. M. Pontekorvo, Zh. Eksp. Teor. Fiz. **33**, 549 (1957) [Sov. Phys. JETP **6**, 429 (1958)]; S. M. Bilenky, B. Pontecorvo, Tbilisi, v. II, B122.
[153]D. C. Cundy, Aachen-Bonn-CERN-London-Oxford-Saclay (BEBC-collaboration) (WA 19/22), "Neutrino-77". P. C. Bosetti *et al.*, Phys. Lett. **B70**, 273 (1977).
[154]A. Bodek, CALTECH-NAL-collaboration, "Neutrino-77". B. C. Barish *et al.*, Phys. Rev. Lett. **39**, 741 (1977).
[155]M. Holder *et al.*, CERN preprint, June 1977 (submitted to Nucl. Instrum. Methods).
[156]R. Turlay, CDHS-collaboration (WAI), "Neutrino-77"; M. Holder *et al.*, Phys. Rev. Lett. **39**, 433 (1977).
[157]A. Benvenuti *et al.*, *ibid.* **38**, 1110, 1183.
[158]H. Mulkens (GGM-collaboration), "Neutrino-77".
[159]D. H. Perkins *et al.*, Phys. Lett. **B67**, 347 (1977).
[160]H. Faissner, in "Neutrino-77".
[161]R. D. Field, R. P. Feynman, Preprint CALT-68-567 (1976).
[162]V. D. Khovanskiĭ (IS-collaboration), "Neutrino-77".
[163]D. J. Fox *et al.*, Phys. Rev. Lett. **33**, 1504 (1974).
[164]E. M. Riordan *et al.*, SLAC-PUB-1634 (1975).
[165]H. L. Anderson *et al.*, Phys. Rev. Lett. **37**, 4 (1976).
[166]H. L. Anderson, Tbilisi, v. II, **B53**.
[167]S. J. Barish *et al.*, ANL-HEP-PR-76-66 (1976).
[168]R. Barbieri *et al.*, Phys. Lett. **B64**, 171 (1976).
[169]M. K. Gaillard, Preprint CERN, TH. 2318 (1977).
[170]G. R. Farrar *et al.*, Phys. Rev. **35**, 1476 (1975); Preprint FNAL 77/45 (1977).
[171]J. T. Dakin *et al.*, Phys. Rev. **D10**, 1401 (1974).
[172]S. J. Barish *et al.*, *ibid.* **D15**, 1 (1977).
[173]M. Holder *et al.*, Phys. Lett. **B69**, 377 (1977); Preprint CERN, July (1977); (submitted to Phys. Lett.).
[174]A. I. Vaĭnshteĭn and I. B. Khriplovich, Usp. Fiz. Nauk **112**, 685 (1974) [Sov. Phys. Usp. **17**, 263 (1974)].
[175]E. P. Shabalin, in Lektsii ITEF (Lectures at the Institute of Theoretical and Experimental Physics), ITÉF-21, M., 1973.
[176]Ya. I. Azimov *et al.*, Usp. Fiz. Nauk **124**, 459 (1978) [Sov. Phys. Usp. **21**, 225 (1978)].
[177]A. I. Vaĭnshteĭn *et al.*, Usp. Fiz. Nauk **123**, 217 (1977) [Sov. Phys. Usp. **20**, 796 (1977)].

Translated by M. V. King